CHEMICAL REVIEWS

REVIEW

pubs.acs.org/CR

Incorporation of Positively Charged Linkages into DNA and RNA Backbones: A Novel Strategy for Antigene and Antisense Agents

Moti L. Jain, Paula Yurkanis Bruice, István E. Szabó, and Thomas C. Bruice*

Department of Chemistry and Biochemistry, University of California, Santa Barbara, California 93106, United States

CONTENTS

1. INTRODUCTION

The discovery, in 1978, by Zamecnik and Stephson[1] that an oligonucleotide can inhibit viral replication in cell cultures ushered in an era of antisense therapeutics. After more than 20 years of experimentation, antisense technology led to the commercialization of the first antisense oligonucleotide drug, Fomivirsen, for cytomegalovirus retinitis.[2] Several others are currently in clinical trials for a wide range of human diseases such cancer, AIDS, hepatitis C, solid tumors, asthma, psoriasis, rheumatoid arthritis, cardiovascular disease, and diabetes.[2−10]

Antigene agents are nucleic acid analogues that function by entering the nucleus of a cell and interfering with the *transcription* of DNA into mRNA (Figure 1). The introduction of a single-stranded antigene agent results in formation of a double-stranded DNA (dsDNA)·antigene triplex that prevents transcription of the target DNA sequence.[11] *Antisense agents* function in the cytoplasm of the cell, where they interfere with the *translation* of mRNA into protein via two common pathways (Figure 1). One pathway involves binding the antisense oligonucleotide to the target mRNA strand, which sterically hinders ribosome binding and therefore mRNA translation. The second pathway involves digestion of the target mRNA by the enzyme RNase H; certain antisense oligonucleotides are adept at recruiting RNase binding to mRNA, facilitating the degradation of the mRNA transcript.

Received: December 17, 2010
Published: November 11, 2011

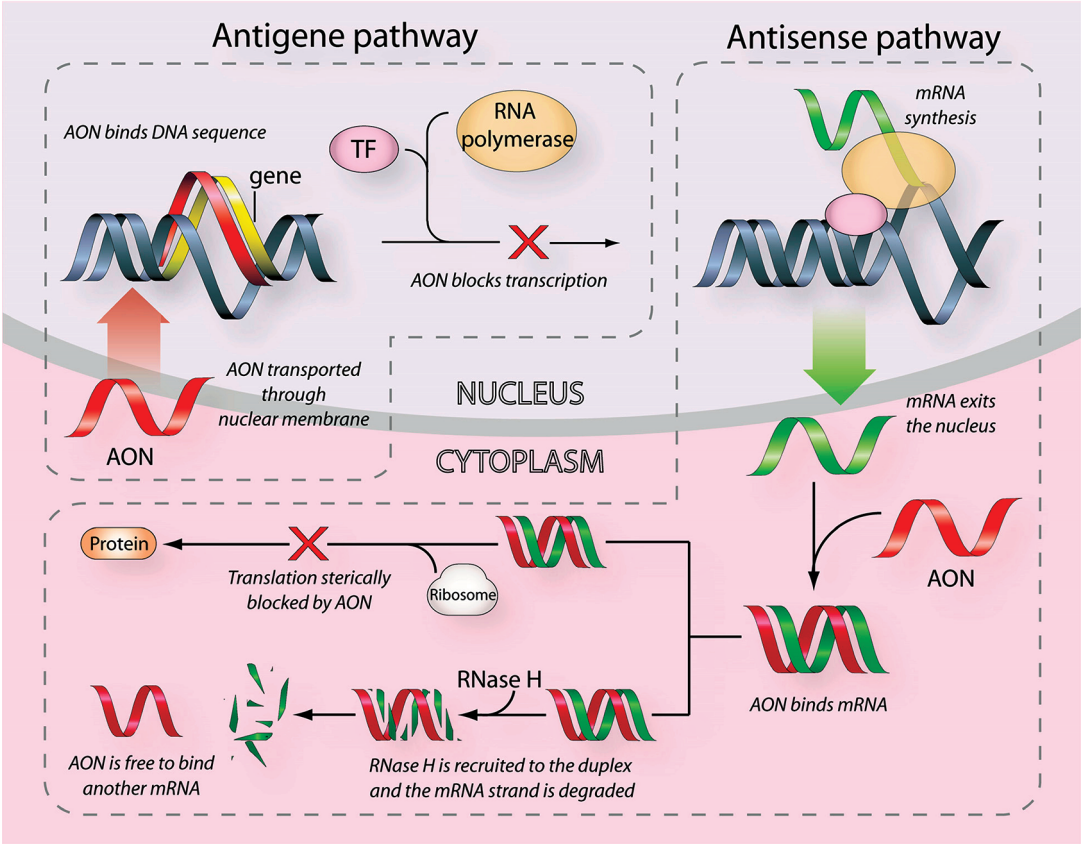

Figure 1. Comparison of antigene and antisense pathways.

In order to be considered effective, antigene/antisense candidates must have a high affinity and specificity for their target DNA or mRNA sequences and must be resistant to degradation by cellular nucleases. The development of antisense/antigene agents should focus on improving the efficacy and drug delivery of these agents, while reducing nonspecific interactions and unwanted side-effects.[7]

The discovery of short interfering RNA (siRNA) initiated a new antisense technology.[12,13] Antisense oligonucleotides (AON) and siRNAs are both short (~20 nucleotides) and are complementary to the target mRNA. There are, however, two significant differences. First, antisense oligonucleotides are single-stranded, whereas siRNAs are double-stranded. Second, antisense oligonucleotides function by binding mRNA, forming an antisense·mRNA duplex that either recruits RNase H (degrading the mRNA) or sterically hinders ribosomal binding (preventing mRNA translation). In contrast, siRNA recognition of mRNA is mediated through an siRNA-induced silencing complex, which subsequently degrades the mRNA target. The studies of siRNAs have been reported in several reviews[14−17] and will not be discussed here.

The major challenges to achieving the therapeutic potential of antisense oligonucleotides are cellular uptake, stability against nuclease degradation in vivo, toxicity, and the binding affinity and specificity of the oligonucleotides.[9,18] To date, many chemically modified oligonucleotides have been synthesized and tested. These are grouped into three categories[2,19,20] (Figure 2): analogues with an altered phosphate backbone (first generation), analogues with a 2′-alkyl substituted ribose ring (second generation), and analogues with modified phosphate linkages, modified ribose rings, or with a completely different chemical moiety replacing the ribose ring (third generation). The first-generation antisense agents have phosphodiester backbone modifications. These include replacement of an oxygen by sulfur (phophorothiolate nucleotides) or methylation of an oxygen (methylphosphonate nucleotides). Phosphorothioate oligonucleotides are the best known and most widely used to date. Their main advantages are resistance to nucleases, ability to recruit RNase H to degrade mRNA, ease of synthesis, and their attractive pharmacokinetic properties. The first FDA-approved antisense drug Vitravene (Fomivirsen) and the majority of the antisense compounds currently in clinical trials are in this class.[2] Their main disadvantages are lower binding affinities and nonspecific interactions that lead to undesirable side effects in vivo, such as immune stimulation and cellular toxicity.[21,22]

The second-generation antisense agents include structures with an electronegative substituent at the 2′-position of the ribose moiety, such as 2′-*O*-methyl and 2′-*O*-methoxyethyl RNA. These substituents confer an RNA-like C-3′-endo conformation to the oligonucleotide that greatly increases its binding affinity.[23] They also show increased nuclease resistance and reduced toxicity. However, these desirable properties are counterbalanced by the fact that these structures do not induce RNase H degradation of target RNA. In order to induce RNase H degradation, mixed-backbone oligonucleotides (known as chimeras) were developed by surrounding a phosphorothioate-modified core that retains RNase H activity with nuclease resistant arms such as 2′-*O*-methyl ribonucleosides.[24−26]

The third-generation antisense agents include a variety of DNA and RNA analogues. Most important among these are the peptide nucleic acids (PNAs),[27−29] the morpholino-phosphoramidates,[30,31]

dx.doi.org/10.1021/cr1004265 |*Chem. Rev.* 2012, 112, 1284–1309

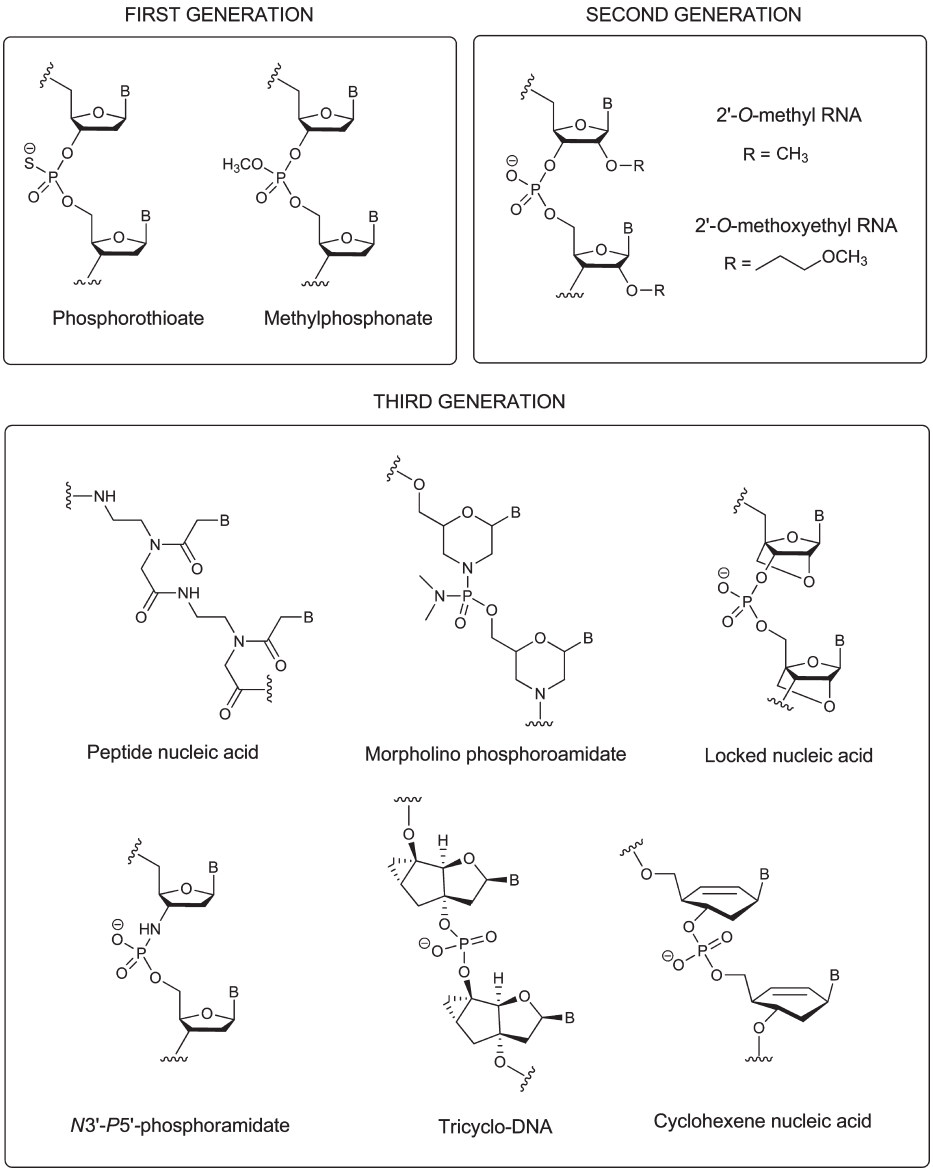

Figure 2. The most common chemically modified nucleic acids (adapted from Kurreck; ref 2).

and the locked nucleic acids (LNAs).[32−36] Neither PNAs nor LNAs (Figure 2) activate RNase H effectively, but they both bind tightly to their RNA targets and most likely exert their effects by blocking translation. The neutral backbone of these agents guards against their binding to proteins that normally recognize polyanions — a major source of the nonspecific interactions of the phosphorothioate oligonucleotides. However, the uncharged backbone causes their solubility and cellular uptake to be major problems.[2]

LNAs possess a methylene bridge that connects the 2′-oxygen of the ribose moiety with the 4′-carbon (Figure 2).[32−36] This induces a conformational change in the DNA·LNA duplex toward the A-type helix and therefore prevents RNase H cleavage of the target RNA.[37] Because LNA bases can be added via standard DNA or RNA synthesis protocols, chimeric "gapmers" can be designed, in which a central DNA portion is flanked by LNA to enhance binding stability. Such LNA-containing oligonucleotides allow the high affinity of LNA binding to be combined with the ability of DNA to recruit RNase H. Most importantly, the enhanced stability of the LNA-containing oligonucleotides against nucleolytic degradation results in a significantly improved half-life in vivo, allowing a longer duration of action. They also do not show acute toxicity.[18] Other important backbone modifications include *N*3′-*P*5′-phosphoroamidates,[38,39] tricyclo-DNA,[40,41] and cyclohexene nucleic acids.[42,43]

2. POSITIVELY CHARGED OLIGONUCLEOTIDES

Several cationic polymers, explored for the purpose of DNA-based drug delivery, have been found to cross the cell membrane, including cationic liposomes,[44,45] polycationic dendrimers,[46] and polyethylenediamine. These are compiled in a review.[47]

The electrostatic repulsion of the two polyanionic chains in dsDNA is balanced by hydrogen bonding between the base pairs and charge screening by counterions. Positively charged oligonucleotide analogues should bind more tightly to DNA with increased association rates. Indeed, several recent studies have shown that the introduction of positively charged groups at different sites in the base,[48−52] sugar,[53−56] or backbone[57−64]

dx.doi.org/10.1021/cr1004265 |*Chem. Rev.* 2012, 112, 1284–1309

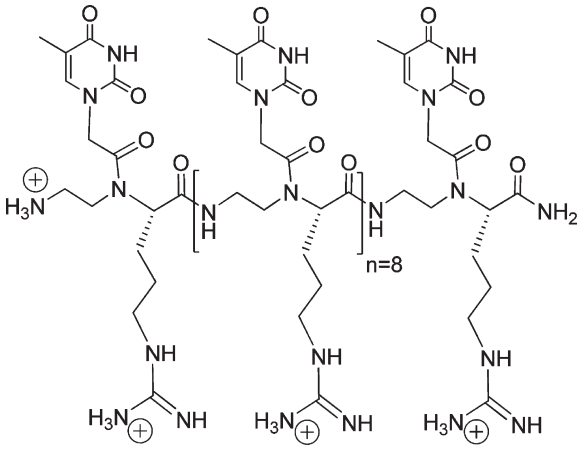

Figure 3. Introduction of arginine side chains into PNA (GPNA-T_{10}).

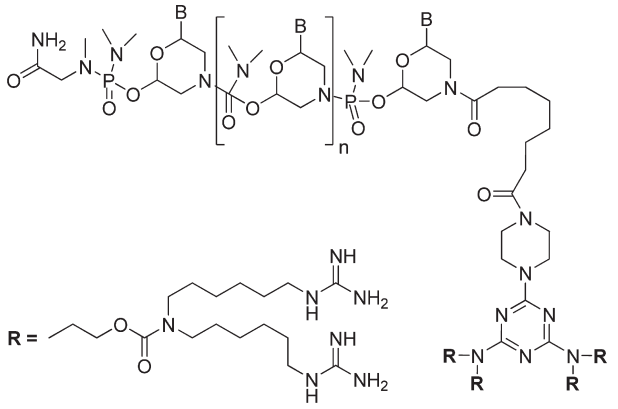

Figure 4. Arginine dendrites on a morpholino backbone.

results in stable duplexes and triplexes.[65] However, when the positively charged group is in the base or the sugar, the duplexes and triplexes are not as stable as those formed when the positively charged group is in the backbone, which is closer to the negatively charged DNA or RNA backbone.

Backbone modifications that retain the chiral phosphorus atom result in complications due to its chirality.[66] Such stereoisomeric constraints apply to a number of cationic backbone-modified oligonucleotides.[63]

Zhou and co-workers reported that incorporation of arginine side chains substituted by guanidinium groups into PNA (Figure 3) results in retention of high sequence specificity and also remarkable cellular uptake properties.[67] PNAs with guanidine side chains are known as GPNAs.

Gene knockdowns have been made using short sequences of morpholino phosphoramidates (Figure 2) to match the DNA target; the morpholino phosphoramidates contain positively charged arginine-rich cell-penetrating peptides that hold the drug and negatively charged DNA in place. One such structure is shown in Figure 4.[68]

The guanidinium group has received special attention because it is achiral, maintains a positive charge over a wide range of pH, and forms both intermolecular hydrogen bonds and intermolecular electrostatic interactions.[69] Pedroso and co-workers prepared oligonucleotides containing a 4-guanidino-2-pyrimidinone nucleoside (Figure 5A), an analogue of protonated cytosine, in the third strand in order to increase triplex stability at neutral

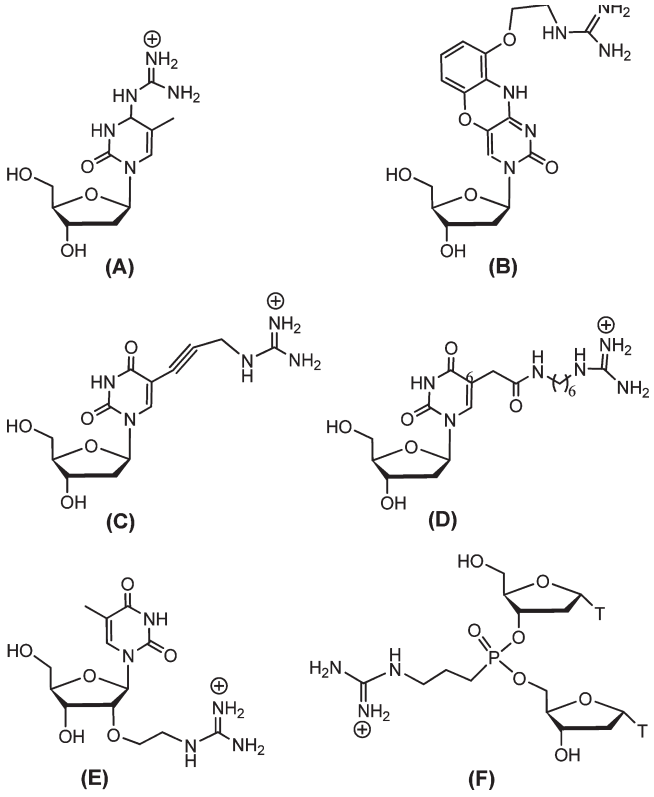

Figure 5. Guanadino-modified nucleosides: (A) 4-guanidino-2-pyrimidinone nucleoside; (B) guanidine G-clamp); (C, D) guanidinium groups tethered to the 5-position of uracil; (E) 2′-*O*-[3-(guanidinium)-propyluridine; (F) guanidinopropylphosphoramidate backbone.

pH.[50] Similarly, the guanidine G-clamp was designed as a cytosine analogue that forms five hydrogen bonds to guanosine (Figure 5B).[70] Linkers ending with guanidinium groups were also introduced at the 5-position of uracil (Figure 5C,D),[51] at the 2′-position of the sugar (Figure 5E),[71] and in the oligonucleotide backbone (Figure 5F)[72] in order to stabilize the triplex. Most importantly, introduction of a guanidinium substituent in these oligonucleotides has been found to improve both cellular uptake and cellular localization.[72] In addition, these nucleotides are highly soluble in water and are nuclease resistant.

3. INCORPORATION OF ACHIRAL POSITIVELY CHARGED GROUPS INTO THE BACKBONE

One way to decrease the free energy associated with the binding of single-stranded DNA (or RNA) with complementary single-stranded antisense oligonucleotides, is to decrease the charge repulsion by designing an antisense oligonucleotide with a positively charged, achiral backbone. Novel replacements for the backbone phosphates include guanidinium [—NHC(=NH_2^+)NH—] linkages and *S*-Methylthiourea [—NHC(=SMe^+)NH—] linkages. An oligonucleotide with guanidinium linkages is called deoxynucleic guanidine (DNG), and one with *S*-Methylthiourea linkages is called deoxynucleic *S*-Methylthiourea (DNmt) (Figure 6).[73−82]

4. OLIGONUCLEOTIDES WITH A GUANIDINIUM BACKBONE

The binding properties and fidelity of base recognition of pentameric thymidinyl DNG was first reported in 1996.[74]

dx.doi.org/10.1021/cr1004265 |*Chem. Rev.* 2012, 112, 1284–1309

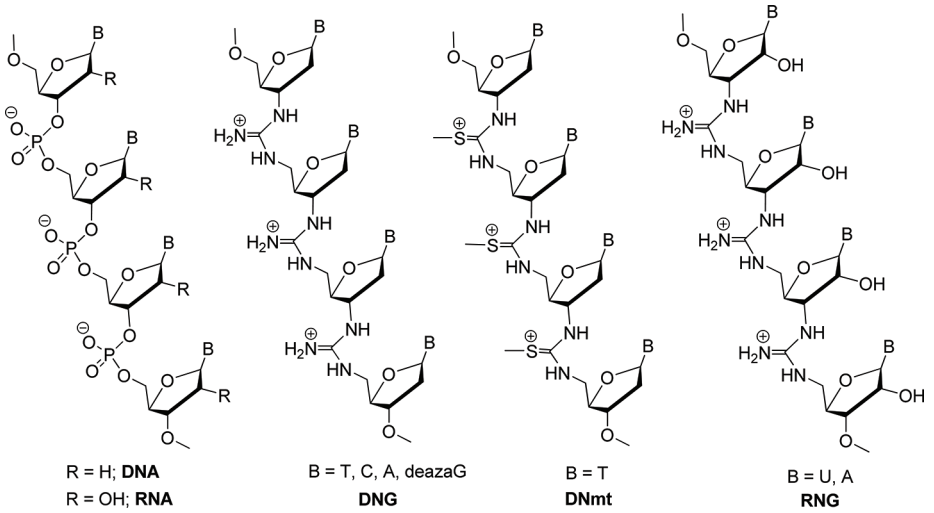

Figure 6. Positively charged DNA and RNA analogues: DNG, DNmt, and RNG.

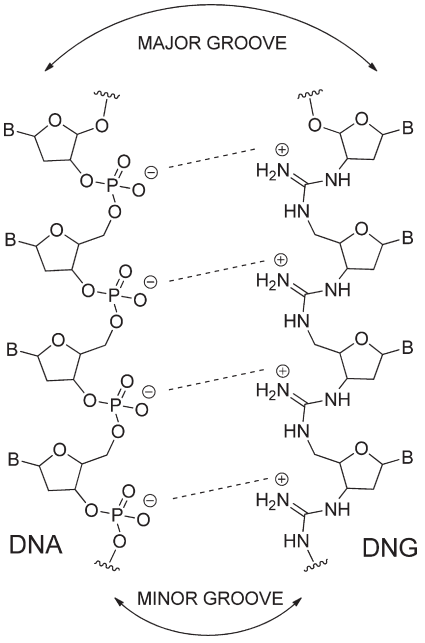

Figure 7. DNA·DNG complex showing the electrostatic attraction between negatively charged phosphodiester linkages and positively charged guanidinium linkages.

Subsequent studies (below) have shown that DNGs have a high binding affinity to DNA due to the proximity of the positive and negative charges (Figure 7), and they bind to DNA with complete base-pair fidelity. In addition, the achiral nature of the linkages in both DNG and DNmt avoids stereoisomeric complexity.

4.1. Synthesis

We prepared polycationic oligonucleotides containing guanidino linkages and bases (A, T, C, and 7-deaza-G). The first synthesis of a pentameric thymidyl DNG (**8**) was carried out in solution in the 5′ → 3′ direction. The synthesis involved preparation of a thiourea dimer (**4**) from 3′-aminothymidine (**1**), chain elongation, followed by oxidation and amidation to give **8** (Scheme 1).[74]

Since the stepwise synthesis of DNG in solution is limited by diminishing coupling yields because of the need for purification at each step, a solid-phase synthesis in the 5′ → 3′ direction was developed.[83] Preparation of octameric thymidyl DNG (**14**), using a commercially available 2-(2-aminoethoxy)ethanol-2-chlorotrityl resin as the solid support, is shown in Scheme 2. The key step is conversion of the thiourea monomer (**10**) to an electronically activated carbodiimide (**11**) by removing sulfur using $HgCl_2/Et_3N$ and coupling with the terminal amine of the growing oligomer to produce a guanidinium linkage (**12**).[84,85] The synthesis was designed to be compatible with standard Fmoc peptide synthesis.

A solid-phase synthesis in the 3′ → 5′ direction was later developed using long chain alkylamine-controlled pore glass (LCAA-CPG) as the solid support, which is compatible with standard solid-phase DNA synthesis.[86] These two methods for solid-phase synthesis allow preparation of DNGs in both the 5′ → 3′ and 3′ → 5′ directions, thus allowing additions to be made at either the 5′- or 3′-end.

Facile routes for preparing the three building blocks (**15**, **16**, and **34**) required for the solid-phase synthesis of a DNG sequence bearing OH groups at both the 3′- and 5′-ends are shown in Schemes 3 and 4. The key step in the synthesis of the capping (**15**) and coupling (**16**) monomers involves inversion of the 3′-OH group of the sugar in order to prepare the xylo-isomer (**18**). Inversion of the 3′-OH group in pyrimidine nucleosides was carried out via a 3′,5′-cyclic derivative by well established procedures;[78,87] 3′-xyloadenine was prepared from a 2′-tosyladenosine derivative.[88,89] For 7-deazaguanine, a novel two-step route was developed that involves Mitsunobu esterification of the 2′-OH group using 4-nitrobenzoic acid and subsequent hydrolysis of the resulting 2′-xyloester.[90]

The capping monomer (**15**) was prepared from the xylonucleoside (**18**) as shown in Scheme 2. Tritylation of the 5′-hydroxy group of **18** formed **19**, which was converted to a 3′-amino derivative (**22**) that, upon treatment with fluorenylmethoxycarbonyl-isothiocyante (FmocNCS),[91] afforded (**15**).[82,90,92] To prepare the coupling monomer (**16**), the xylonucleoside (**18**) was converted to a diamino derivative (**27**). The regioselective tritylation of the 5′-amino group of **27** and its subsequent reaction with FmocNCS afforded **16**. The loading monomer (**33**) was prepared from the nucleoside and loaded onto a CPG support as a 3′-succinyl

dx.doi.org/10.1021/cr1004265 |*Chem. Rev.* 2012, 112, 1284–1309

Scheme 1[a]

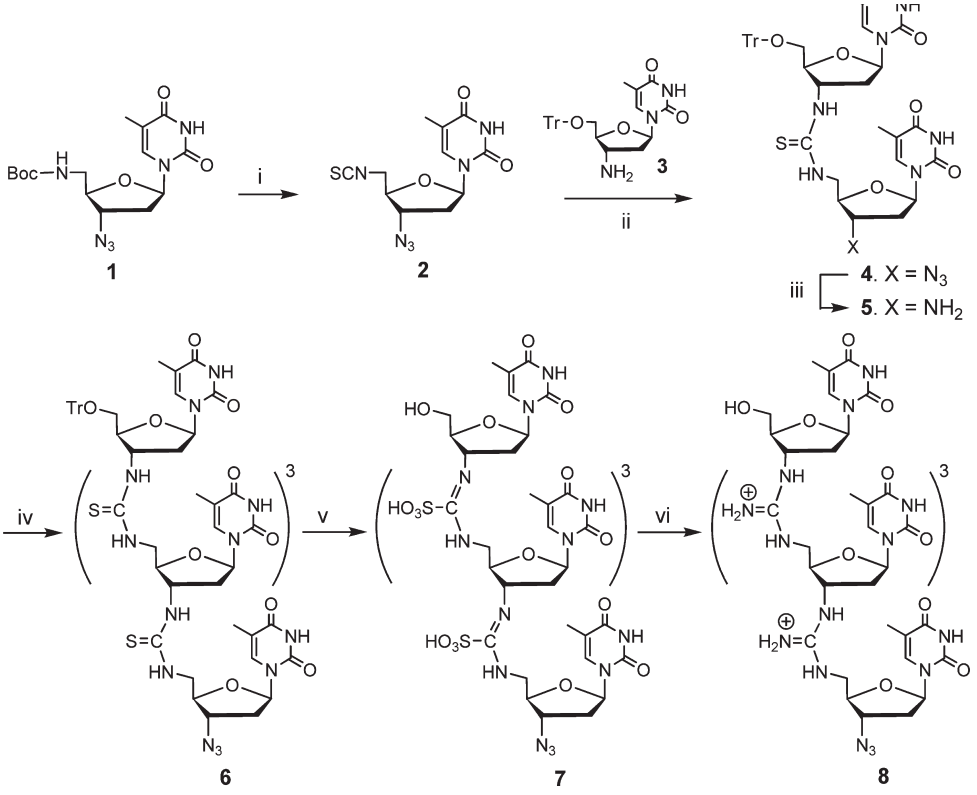

[a] Reagents and conditions: (i) (1) trifluoroacetic acid, CH_2Cl_2, (2) CS_2, DCC DMF; (ii) **3**, DMF; (iii) H_2S(g), aq. pyridine; (iv) repeat steps (ii) and (iii) twice; (v) (1) TFA, CH_2Cl_2 (2) peracetic acid (32%) in acetic acid; (vi) NH_4OH.

ester (**17**) using a standard 4-nitrophenol/DCC protocol.[81,82,92] More recently, 4-(4,6-dimethoxy-1,3,5-triazin-2-yl)-4-methylmorpholinium chloride (DMTMM)[93] was used as the coupling agent and gave excellent loading yields (Scheme 4).[90] A typical synthesis of the guanidinium linkage involves in situ generation of a carbodiimide from a Fmoc-protected thiourea using $HgCl_2/Et_3N$ and its subsequent coupling with amine (Figure 8).[82,86,90,92]

The solid-phase synthesis of DNG was carried out in the 3′ → 5′ direction (Scheme 5). After the MMTr protecting group was removed from the 5′-position of (**34**), the liberated amine was coupled with the activated carbodiimide of the incoming coupling monomer (**16**) (the synthesis of **16** is shown in Scheme 3) to generate a protected guandinium-linked dimer (**36**). The two-step deblocking/coupling process was repeated to prepare a DNG of the desired length. The final coupling was carried out with the capping monomer (**15**) to provide a terminal OH group. Finally, cleavage from the solid support and removal of the protecting groups gave the desired DNG oligonucleotide (**39**). The coupling yields were 90−98%. Most importantly, the presence of free 5′- and 3′-OH groups (as in **39**) allows the synthesis of a DNG/DNA chimera of any desired sequence.[82,90]

4.2. Binding and Thermal Denaturation Studies

Job plot analyses show that DNG-T_5 (**8** in Scheme 1) forms a triple-stranded complex with DNA-A_{poly} or with RNA-A_{poly}. These triplex structures are represented as (DNG-T_5·DNA-A_{poly})·DNG-T_5 and (DNG-T_5·RNA-A_{poly})·DNG-T_5.[74,76,79,80] In addition, DNG-A_5 forms a triple-stranded complex with DNA-T_5, represented by (DNA-T_5·DNG-A_5)·DNA-T_5.[86] Thus, each triplex contains two T strands and one A strand regardless of whether the T strand is a DNG or a DNA. In the case of cytidinyl[92] and 7-deazaguanyl[90] DNGs, the binding stoichiometry is 1:1, indicating the formation of complementary base-paired DNG·DNA duplexes. Figure 9 shows a Job plot for the 2:1 binding of DNG-T_8 to RNA-A_{poly}.[83] Figure 10 shows the 1:1 binding of DNG-C_6 to DNA-G_6.[92]

A DNG-T interacts with a DNA-A to form double-stranded complexes DNA-A·DNG-T and triple-stranded complexes (DNA-A·DNG-T)·(DNG-T). Similar complexes are formed between RNA-A and DNG-T (whereas DNG-C and DNA-G form only a mixed duplex).[81]

The thermal stabilities for various combinations of DNG and DNA, at various ionic strengths, are shown in Figure 11. With increasing ionic strength, DNA·DNA and DNA·RNA duplexes become somewhat more stable. This is not unexpected, since an increase in ionic strength will stabilize dsDNA or DNA·RNA by masking the repulsive negative charges. In contrast, an increase in ionic strength allows the oppositely charged strands of DNG·DNA or DNG·RNA to be less closely paired and thereby destabilized.[74,76,79] Notice that the DNG·DNA duplex is dramatically more stable than the DNA·DNA duplex at physiological ionic strength. This is a desired property for antisense/antigene agents.

The thermal stabilities of DNG complexes with DNA are greater than those of a number of DNA complexes with other synthetic entities.[51,71,72,76,81,86,92] In general, a base mismatch at the center of a DNA sequence decreases the T_m significantly, due to the shorter length of the matched paired bases. A base mismatch at either end of a sequence has less of an effect on

dx.doi.org/10.1021/cr1004265 |*Chem. Rev.* 2012, 112, 1284–1309

Scheme 2[a]

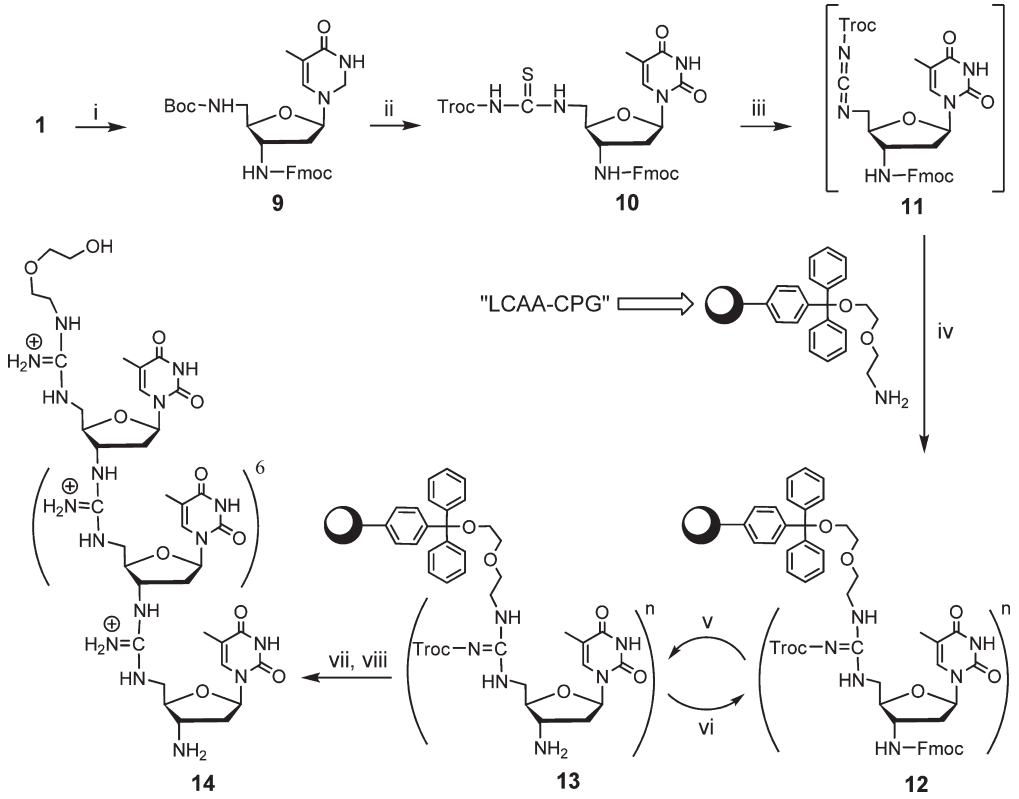

[a] Reagents and conditions: (i) (1) Pd/C, H_2, EtOH; (2) Fmoc-Cl, 10% Na_2CO_3, dioxane; (3) TFA, CH_2Cl_2; (ii) Troc-NCS, CH_2Cl_2; (iii) $HgCl_2$, TEA, DMF; (iv) resin; (v) deprotection: 20% piperidine in DMF; (vi) coupling: monomer **8**, $HgCl_2$, TEA, DMF, and cycle repeated six more times; (vii) cleavage: 3% dichloroacetic acid in CH_2Cl_2; (viii) deprotection: AcOH, zinc powder.

stability, because the length of the matched sequence is less affected. For example, the T_m of a 2:1 complex of DNG-T_8 with cDNA-A_8 drops from 63 to 55 °C when two **C** mismatches are introduced at the ends (**C**A_6**C**). A single base mismatch at the center (A_4**C**A_3) results in a sharp decrease in QT_m to 48 °C, and two central base mismatches (A_3**CC**A_3) completely eliminate the base-pairing association.[81]

We envision that positively charged DNGs or mixed-charged DNG/DNA chimeras, because of their base pairing fidelity and tight binding, can be ideal inhibitors of negatively charged DNA and RNA targets. An added advantage is that the tightness of the binding can be controlled by the number of guanidine linkages in the chimera or by base mismatches.

4.3. Circular Dichromism Spectral Studies[75]

The CD spectrum of an oligonucleotide in solution provides valuable information about its conformation. The CD spectrum of ssDNG-T_8 is very different from that of ssDNA-T_8. The angle between the bonds of the tetrahedral phosphate is ~109°, whereas the angle between the bonds of a guanidinium group is ~120°. This wider bond angle increases the distance between the bases in ssDNG; consequently, the bases do not stack as effectively as in ssDNA. However, the CD spectrum of the triple-helical complex (DNG-T_8)$_2$·DNA-A_8 indicates a normal B-DNA triple helix.

4.4. Comparison of the Binding of DNA to DNG with the Binding of DNA to DNA

Plasmodium falciparum, the parasite responsible for malaria, is rich in $(AT)_n$ sequences. In contrast, $(AT)_n$-rich sequences are rare in human DNA. Therefore, a starting point for assessing the potential of DNG/DNA chimeras as therapeutic agents is to evaluate their binding to model targets with $(AT)_n$-rich sequences. (A chimera is a single-stranded oligonucleotide with mixed backbone linkages and is indicated by a forward slash. Thus, DNG/DNA is a single strand that contains both guanidinium and phosphate linkages.) One such target is based on the bacterial juvenile esterase gene (JEG).[94]

We examined the free energy of binding of a 20-mer DNA sequence of the juvenile esterase gene (JEG-20) to a complementary 20-mer DNA sequence to form duplex **1**. We also examined the free energy of binding of JEG-20 to a complementary 20-mer DNG/DNA chimera to form duplex **2**.[95]

GCGTGCGTpApTpApTpAACACGCC	JEG-20	
CGCACGCApTpApTpApTTGTGCGG	complementary DNA	**duplex 1**
GCGTGCGTpApTpApTpAACACGCC	JEG-20	
CGCACGCAgTgAgTgAgTTGTGCGG	complementary DNG/DNA chimera	**duplex 2**

The binding of the chimera shows complete sequence specificity. The ratio of the equilibrium constants indicates that binding of the chimera to JEG-20 is more than 10^6 times stronger than binding of the DNA to JEG-20. This ratio becomes less if one or two changes are made in the DNA sequence of the chimera.

Scheme 3[a]

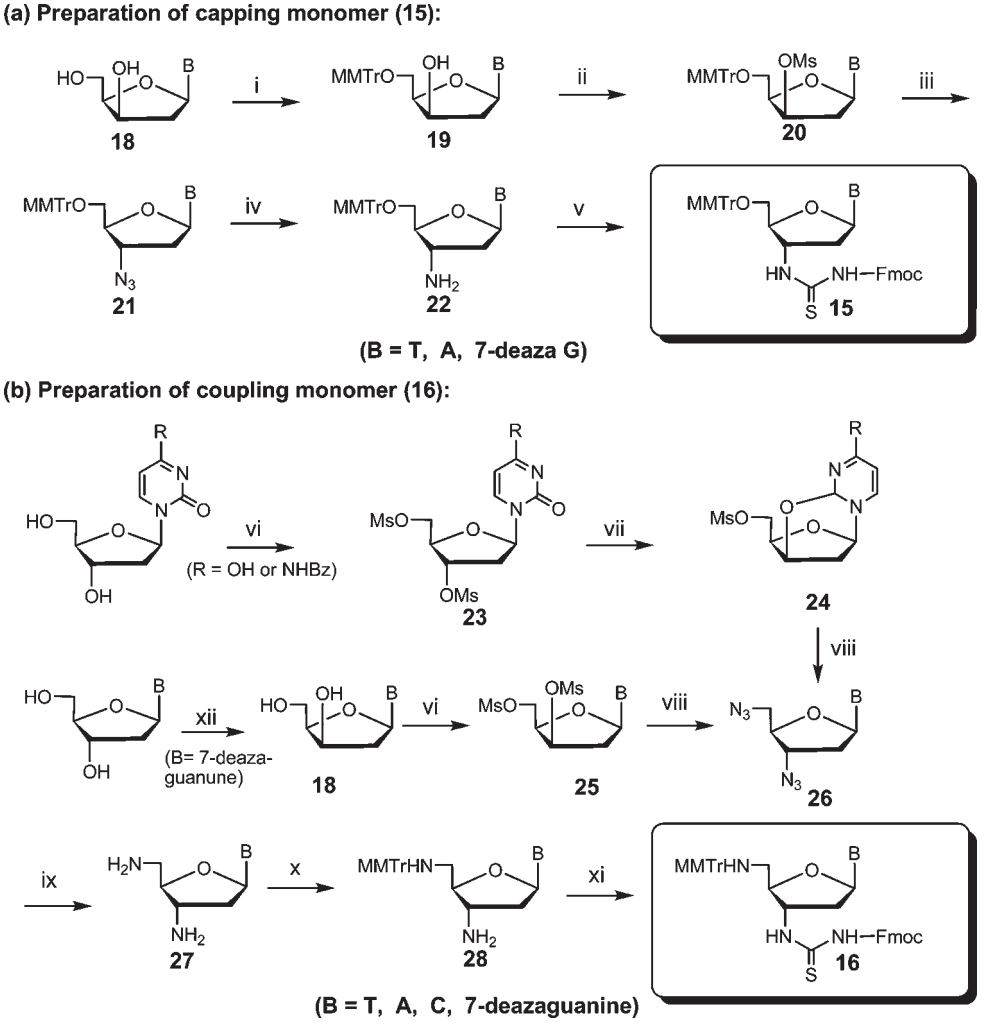

[a] Reagents and conditions: (i) MMTrCl, pyridine, rt; (ii) CH_3SO_2Cl, pyridine, 0 °C to rt; (iii) LiN_3, DMF, 80 °C; (iv) 10% Pd/C, H_2, EtOH; rt; (v) Fmoc-NCS, CH_2Cl_2, rt; (vi) CH_3SO_2Cl, pyridine, 0 °C to rt; (vii) potassium phthlamide, DMF, 100 °C; (viii) LiN_3, DMF, 80 °C (ix) 10% Pd/C, H_2, EtOH, rt; (x) MMTrCl, TEA (or DEA, CH_2Cl_2, rt; (xi) Fmoc-NCS, CH_2Cl_2, rt; (xii) (a) 4-nitrobenzoic acid, DIAD, PPh_3, THF, rt; (b) NH_3/MeOH, rt.

Scheme 4[a]

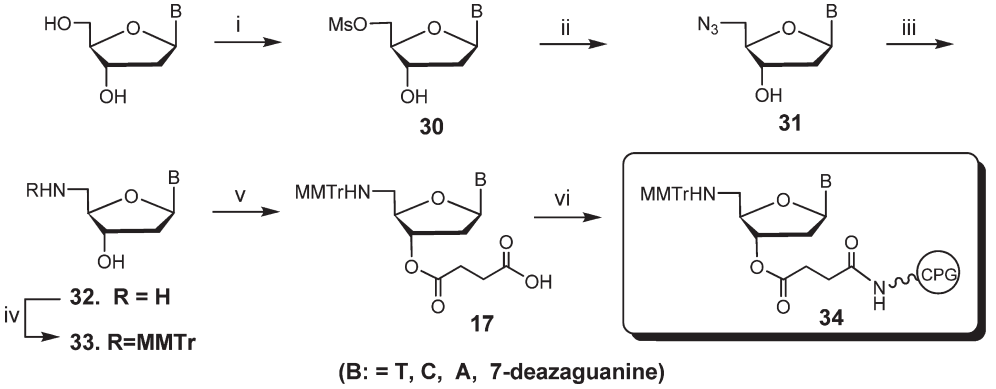

[a] Reagents and conditions: (i) CH_3SO_2Cl, pyridine; (ii) LiN_3 DMF, 80 °C; (iii) 10% Pd/C, H_2, EtOH; (iv) MMTrCl, pyridine; (v) succinic anhydride, DMAP, pyridine; (vi) 4-nitrophenol, DCC, pyridine (or MMTMM, MeOH in case of 7-deazaguanine), LCAA-CPG.

dx.doi.org/10.1021/cr1004265 |Chem. Rev. 2012, 112, 1284–1309

Because A and T guanidinium-linked bases are easy to prepare and the polycationic AgTgAgTgAgT binds tightly to its complementary polyanionic DNA sequence (TpApTpApTpA), it gives us readily accessible inexpensive starting materials with which to build chimeras.

TgAgTgAgTgA--------DNA

DNA----------ApTpApTpApT

4.5. Telomerase Inhibition by Oligonucleotides

Oligonucleotides have also been explored as inhibitors of the human telomerase enzyme for cancer therapy. Telomerase is responsible for the synthesis of the hexanucleotide [d(5′-TTAGGG-3′)$_n$] repeats (telomeres) at the 3′-end of a dividing chromosome (Figure 12). Human telomeric DNA consists of repeats of the sequence (5′-TTAGGG-3′) on one strand and a complementary sequence on the matching strand (3′-AATCCC-5′). The telomere single strands serve as a substrate for telomerase, the enzyme that rebuilds the telomere strand lost during cell division. Telomerase consists of a reverse transcriptase with an 11-base RNA template (5′-CUAACCCUAAC-3′) at the active site.

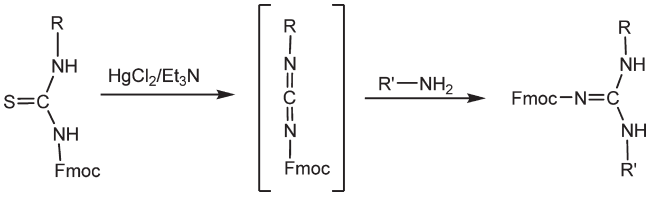

Figure 8. Formation of carbodiimide and subsequent addition to form the protected guanidino group.

Because telomerase is expressed in nearly 90% of human tumor cells but is not expressed in most normal somatic cells, both telomerase and the telomere have been extensively targeted for cancer therapeutics.[96] Several oligonucleotides have been prepared and evaluated as inhibitors of telomerase. These include phosphorothioates,[97,98] phosphoramidates,[99] 2′-*O*-methyl- and 2′-*O*-methoxyethyl-phosphorothioate chimeras,[100] and PNAs.[98] Senescence and the subsequent death of tumor cells caused by these telomerase inhibitors are observed only in cells with short telomeres. About 50−100 base pairs are lost in each round of replication. Thus, for telomeres with an average length of 5 kb, about 50 rounds of replication must occur before the onset of

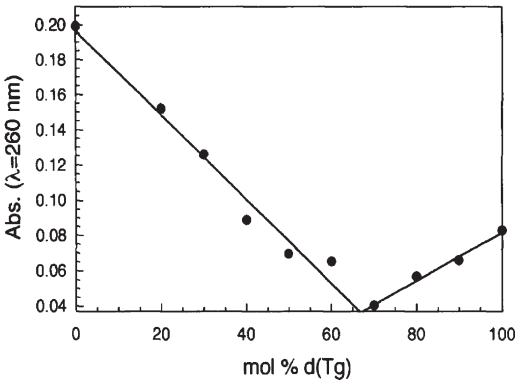

Figure 9. Job plot (continuous variation method) of RNA-A$_{poly}$ with **7**, at λ = 260 nm and 30 °C. Inflection at 67% indicates 2:1 DNG/DNA complex. Reprinted with permission from ref 83. Copyright 1998 Elsevier.

Scheme 5[a]

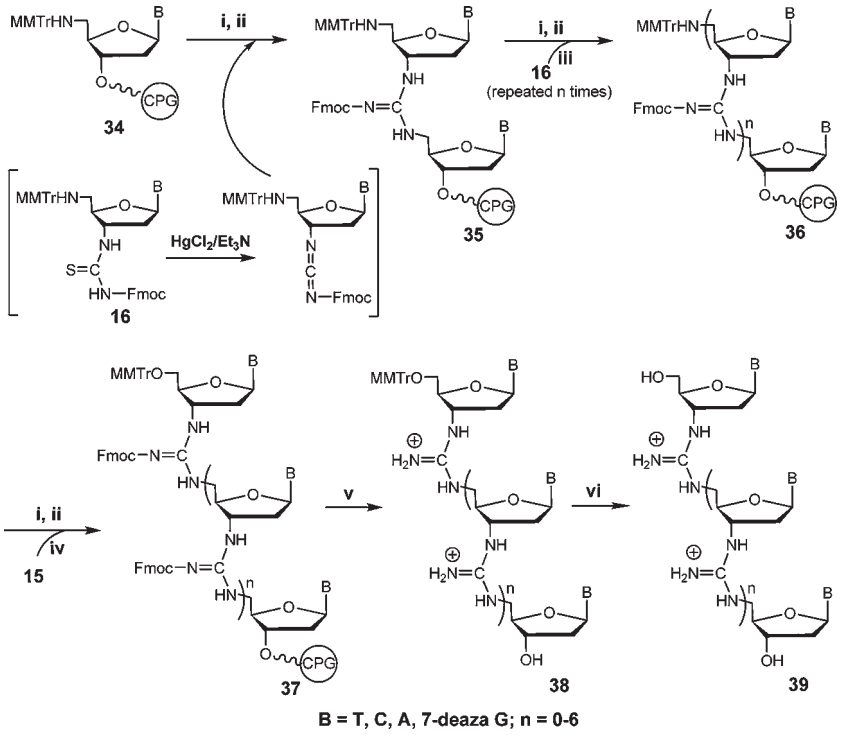

[a] Reagents and conditions: (i) capping: Ac_2O, TEA, DMF, 10 min; (ii) deprotection: 3% dichloroacetic acid in CH_2Cl_2, 1 min; (iii) coupling: monomer **16** $HgCl_2$, TEA, DMF, 2 h, then 20% PhSH in DMF, 1 min; (iv) coupling: monomer **15**, $HgCl_2$, TEA, DMF, 2 h, then 20% PhSH in DMF, 1 min; (v) NH_4OH, 60 °C, 15 h; (vi) 3% dichloroacetic acid in CH_2Cl_2, 1 min.

dx.doi.org/10.1021/cr1004265 |*Chem. Rev.* 2012, 112, 1284–1309

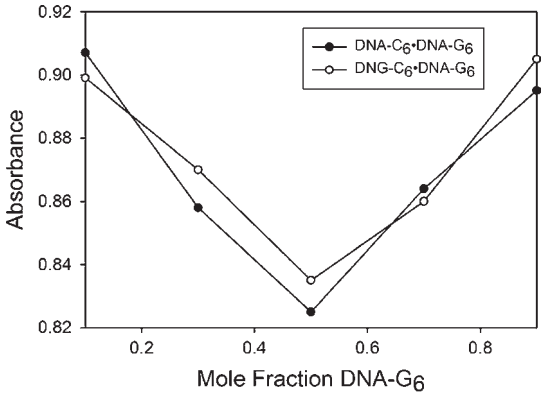

Figure 10. Job plot illustrating 1:1 binding of DNA-C_6, and DNG-C_6, to DNA-G_6. Total oligomer concentration was 12 mM and buffer contained 100 mM [KCl], 10 mM [$KHPO_4$], adjusted to pH 7. Reprinted with permission from ref 92. Copyright 2004 Elsevier.

senescence. This implies an extensive lag time before senescence can occur, indicating that anti-telomerase drugs might be beneficial only for tumor cells with short telomeres.[101] One telomerase inhibitor, a lipid-conjugated 13-mer thiophophoramidite, GRN 163 L (5′-pam-TAGGGTTAGACAA-NH_2-3′) developed by Geron Corporation (USA), is in phase I/II for chronic leukemia and breast cancer.[102]

Another approach involves complexing the single-strand telomeric 3′-overhang $(TTAGGG)_n$, which in humans averages 130–210 bases in length,[103] so that it cannot be propagated either by telomerase or by DNA polymerase, thus leading to tumor cell death. This alternative strategy is independent of telomere length and therefore eliminates the lag phase associated with telomerase inhibition. We envision that positively charged DNGs could be ideal inhibitors of the negatively charged DNA and RNA targets.

4.6. The Telomeres and the Active Site of Telomerase

The free energies for binding DNGs to telomeric sequences were calculated by computer simulations[104] employing implicit solvent model and Generalized Born molecular volume (GBMV)[105,106] (Figure 13). The calculated free energy for binding complementary DNG (3′-AgAgTgCgCgCg-5′) to the DNA telomeric sequence (5′-TpTpApGpGpGp-3′) exceeds that for binding cDNA (3′-ApApTpCpCpCp-5′) to the telomeric sequence by 8.3 kcal/mol ($\sim 10^6$-fold). The strength of duplex binding decreases if the number of guanidine linkages decreases. For example, a chimera with three DNG units and three DNA units (3′-ApAgTpCgCpCg-5′) has been calculated to bind more tightly to the telomeric sequence than does DNA by 5.6 kcal/mol ($\sim 10^4$-fold). In addition, both DNG and the DNG/DNA chimera bind more tightly to the telomeric sequence than does human telomerase.[107]

DNG/DNA I (AgAgTgCgCpCp) was synthesized, and the stability of the duplex it forms with cDNA in water was determined by thermal denaturation experiments (pH 7.0, 0.1 M NaCl).[108] This chimera, with four guanidinium linkages, was found to bind to cDNA much more tightly (by 3.5 kcal/mol, $\sim 10^{2.5}$ fold) than DNA binds to DNA in dsDNA.

TpTpApGpGpGp	**DNA**
AgAgTgCgCpCp	**DNG/DNA I**

The melting temperature of the duplex formed with 10 guanidinium linkages (**DNG/DNA II**) and cDNA (with a sequence of two telomeric repeats) could not be determined because they bind too tightly to allow dissociation. Thus, not surprisingly, the binding strength is increased by extending the length of the DNG block in the (DNA/DNG)·DNA duplex.

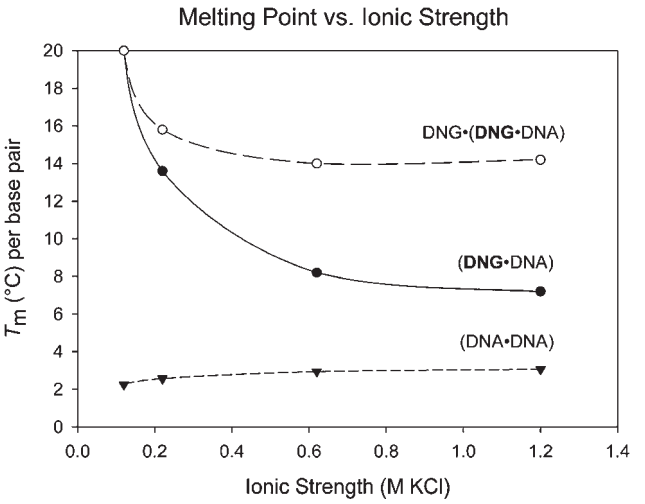

Figure 11. Thermal stabilites (T_m) of the complexes, DNA·DNG, DNA·DNG_2, and dsDNA at pH = 7 and various ionic strengths (μ) [DNA = DNA-A_{poly} and DNG = DNG-T_5]. The thermal stabilities of complexes involving DNA·DNG interaction reach a maximum at the physiological ionic strength of μ = 0.11 M, whereas DNA·DNA bonding is minimal at this value.

TpTpApGpGpGpTpTpApGpGpG	$(telomere)_2$
AgAgTgCgCgCgAgAgTgCgCpC	**DNG/DNA II**

DNG binds to both DNA and RNA, but it exhibits a marked preference for RNA.[104,108] The unprecedented high binding affinity of complementary DNGs for both RNA and DNA clearly demonstrates that both DNG centered antisense oligonucleotides and targets for the RNA template in telomerase will be found.

5. OLIGONUCLEOTIDES WITH AN *S*-METHYLTHIOUREA BACKBONE[109−113]

To further investigate the properties of positively charged linkages, oligonucleotides with *S*-Methylthiourea linkages (DNmts) were prepared (Figure 6). These linkages, while retaining the positive charge of the DNG linkage, also have some of the backbone structural features of the phosphorothioate and methylphosphonate oligonucleotides (Figure 2).

5.1. Synthesis

The solid-phase synthesis of pentameric thymidyl DNmt (**43**) was carried out in the 3′ → 5′ direction (Scheme 6). The coupling monomer (**40**) was prepared from the corresponding 3′-amino derivative (**22**). The 5′-MMTr protecting group of **34** was removed, and the resulting amine was coupled with monomer **40** to give the thiourea dimer (**41**). The deblocking/coupling steps were repeated three more times to yield **42**. Methylation of the thiourea groups of **42** followed by cleavage from the support and removal of the MMTr-group gave the desired DNmt-T_5 (**43**). The coupling yields were ~87%.

5.2. Binding and Thermal Denaturation Studies[109−112]

Job plots in aqueous solutions of DNmt-T_5 in the presence of cDNA-A_{poly} or RNA-A_{poly} show formation of the following

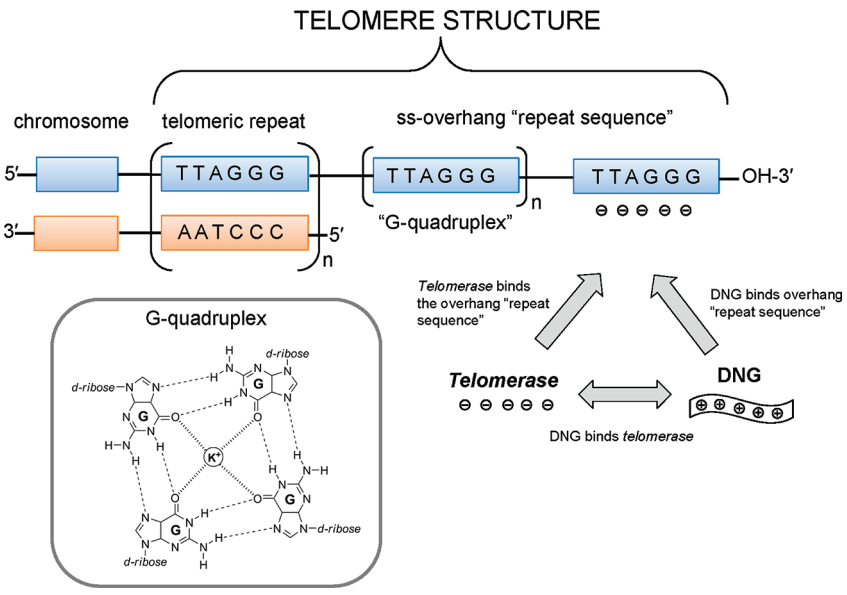

Figure 12. Structure of the telomere that is found at the end of chromosomes. The structure of the G-quadruplex, which consists of a single strand repeat of 5′-TTAGGG-3′, is shown in the boxed inset. The single-ended arrows show the association of telomerase and DNG for the overhang "repeat sequence", and the double-headed arrow indicates the binding of DNG to telomerase.

triple-stranded complexes: (DNA-A_{poly}·DNmt-T_5)·(DNmt-T_5) and (RNA-A_{poly}·DNmt-T_5)·(DNmt-T_5).

Like positively charged DNG-T_5, positively charged DNmt-T_5 exhibits a much greater affinity than does DNA-T_5 for DNA-A_{poly} or for RNA-A_{poly}. At physiological pH and μ = 0.12 M, the T_m for the DNmt-T_5·DNA-A_{poly} duplex is >80 °C, whereas that for the DNA-T_5·DNA-A_{poly} duplex is only 13 °C. At higher ionic strength (μ = 0.3 M), DNmt-T_5·DNA-A_{poly} exhibits two distinct inflections at 35 and 65 °C. These correspond to denaturation of the (DNmt-T_5·DNA-A_{poly})·DNmt-T_5 triplex and the DNmt-T_5·DNA-A_{poly} duplex, respectively. In the case of (DNmt-T_5·RNA-A_{poly})·DNmt-T_5, only one inflection is observed (T_m = 65 °C, μ = 0.15 M and T_m = 85 °C, μ = 0.03 M), which represents the melting point of the triplex (DNmt-T_5·RNA-A_{poly})·DNmt-T_5. Therefore, DNmt-T_5·RNA-A_{poly})·DNmt-T_5 is more stable than (DNmt-T_5·DNA-A_{poly})·DNmt-T_5. Binding is highly specific to complementary tracts of adenine bases; DNmt-T_5 does not bind to guanyl, cytidyl, or uridyl bases. Similarly, no hyperchromic shift is seen with solutions that contain DNmt-T_5 and either RNA-U_{poly}, RNA-C_{poly}, or RNA-G_{poly}.

The (DNmt-T_5·DNA-A_{poly})·DNmt-T_5 and (DNmt-T_5·RNA-A_{poly})·DNmt-T_5 triplexes, like the DNG complexes in Figure 11, are more stable at low ionic strength. At any ionic strength, the (DNmt-T_5·RNA-A_{poly})·DNmt-T_5 triplex is more stable than the (DNmt-T_5·DNA-A_{poly})·DNmt-T_5 triplex. Furthermore, in spite of its high binding affinity, DNmt-T_5 exhibits high base-pair specificity when forming a triple helix with DNA-A_{20}.[112] There is a sharp decrease in T_m with an increase in the base mismatch with DNA: the T_m of the (DNmt-T_5·DNA-A_{poly})·DNmt-T_5 triple helix drops from 48 to 39 °C when complexed with DNA that has a 20% **C** mismatch (5′-**C**A_4**C**A_4**C**A_4**C**A_3A-3′) and drops to <20 °C with DNA that has a 50% C mismatch (5′-**CACACACACACACACACACA**-3′).

All oligonucleotides with positively charged linkages bind more tightly to DNA than does DNA. The increase in melting temperature for the DNG·DNA duplexes near physiological conditions (μ = 0.12 M, pH 7) (T_m/bp = ~15−25 °C) are comparable to that observed for the DNmt·DNA duplexes (T_m/bp = ~15 °C) but higher than that for DNA duplexes with ethylmorpholino phosphoramidate, aminoethylphosphonate (T_m/bp =2−3 °C),[61] or 2′-*O*-aminopropyl (T_m/bp = ~3.5 °C) modified oligonucleotides.[71] This suggests that DNmt, like DNG, maintains its positive charge in an alignment that maximizes its interaction with the phosphodiester backbone of DNA.

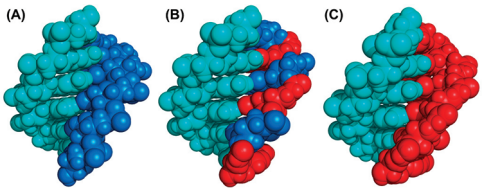

Figure 13. The average structures from 4 ns MD simulations of (A) telomere·DNA (TpApGpGpGpT·ApTpCpCpCpA), (B) telomere·chimera (TpApGpGpGpT·AgTpCgCpCgT), (C) telomere·DNG (TpApGpGpGpT·AgTgCgCgCgA). Telomeres are cyan, DNA nucleotides are blue, and DNG nucleotides are red.

5.3. Circular Dichromism Studies[112]

Further evidence for the base-pair specificity of DNmt-T_5 binding is evident from CD spectra. Clear differences can be seen in the binding of DNmt-T_5 to cDNA-A_5 and to DNA containing mismatched bases (Figure 14). The negative signal at 250 nm gradually disappears and the positive signal at 212 nm decreases on going from oligo **1** to oligo **5**. The spectral drop in amplitude is an indication that the degree of association between the oligomers and DNmt strands is weakening as the number of mismatches increases.

5.4. Molecular Dynamic Simulations

Molecular dynamic studies of DNG-T_8·DNA-A_8 and DNmt-T_8·DNA-A_8 duplexes as well as (DNA-A_8·DNG-T_8)·(DNG-T_8) and (DNA-A_8·DNmt-T_8)·(DNmt-T_8) triplexes establish an overall B-DNA conformation.[114,115] These studies show, as do

dx.doi.org/10.1021/cr1004265 |*Chem. Rev.* 2012, 112, 1284–1309

Scheme 6[a]

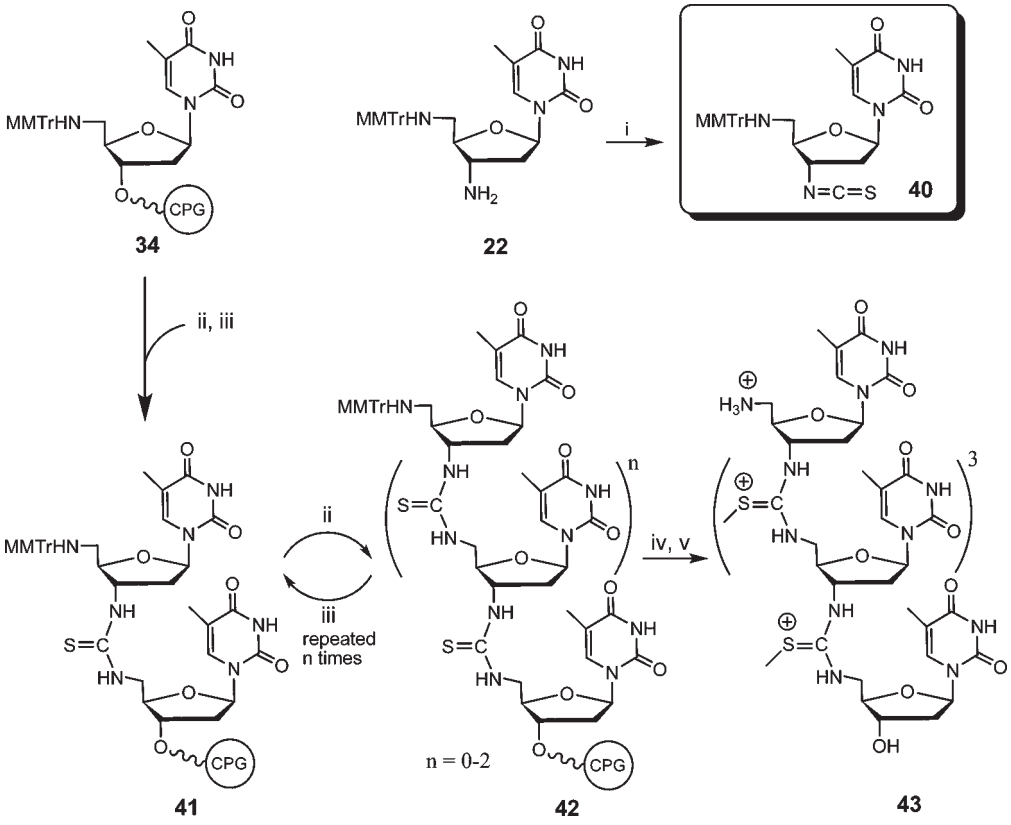

[a] (i) Thiocarbonylpyridone, CH_2Cl_2, rt; (ii) deblocking; 4% dicloroacetic acid in CH_2Cl_2; (iii) coupling; (**40**), DMAP, pyridine, rt; (iv) CH_3I, EtOH; (v) NH_4OH, rt. CPG = control pore glass.

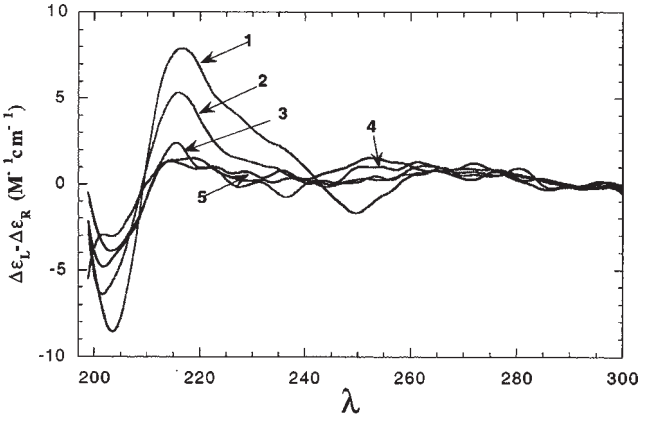

Figure 14. Difference CD spectra for triplexes formed from the binding of DNA oligomers (**1**−**5**) to DNmt. The ratio of DNA/DNmt was 1:2. Reprinted with permission from ref 112. Copyright 1999 American Chemical Society.

our thermodynamic studies, that in solution at ambient temperature, triplex formation is more favorable than duplex formation.

A notable structural feature of the DNG-T_8·DNA-A_8 and DNmt-T_8·DNA-A_8 duplexes, compared to the DNA·DNA duplex, is a narrower minor groove (0.7 Å) due to attraction between the oppositely charged backbones of DNA and DNG. The narrower minor groove induces a wider major groove, which provides more space for a third strand.[114,115]

The bases are farther apart in triplexes formed by dsDNA with DNG[114] (or DNmt)[115] than they are in DNA; the overall elongation with is 0.2 Á between base pairs. This elongation is compensated by a widening of the minor groove because of the oppositely charged backbones of DNA and DNG (or DNmt). Therefore, the minor groove width of the triplexes is the same as that of dsDNA.[114,115]

The triplexes formed by DNG or DNmt with dsDNA show greater ease in bending than does the DNA triplex. The bending features of DNA are important in transcription, replication, and other processes.[116,117] Bending is more pronounced in DNG (30°) than in DNmt (20°), because of the different charge distributions in the two linkages (Figure 15).[115] The structures in Figure 15 are theoretical models[118] that have been graphically represented using MidasPlus.[119]

6. OLIGONUCLEOTIDES WITH MIXED BACKBONES

Unfortunately, most of the modifications that cause an antisense polymer to be resistant to hydrolysis by nucleases also prevent it from being a substrate for RNase H when the polymer is complexed with RNA. All known modifications, including backbone replacements (such as morpholinos and PNAs), most phosphate modifications (such as phosphoramidates and methylphosphonates), and 2′-ribose modifications, do not form a substrate for RNase H when complexed to RNA.[120]

The most commonly used approach for overcoming the lack of RNase H recruitment involves preparation of mixed-backbone

dx.doi.org/10.1021/cr1004265 |*Chem. Rev.* 2012, 112, 1284–1309

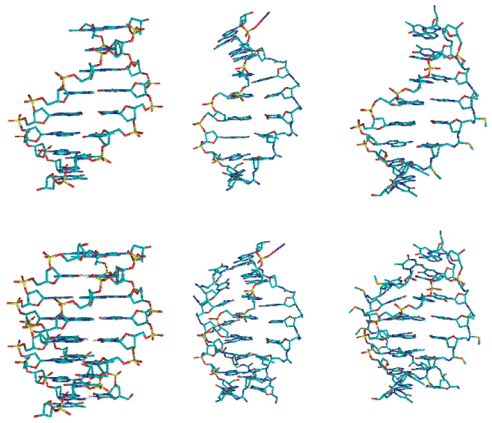

Figure 15. Structures from left to right: (top) DNA-T_8·DNA-A_8, DNG-T_8·DNA-A_8 and DNmt-T_8·DNA-A_8 duplexes; (bottom) DNA-T_8·DNA-A_8·DNA-T_8, DNG-T_8·DNA-A_8·DNG-T_8, and DNmt-T_8·DNA-A_8·DNmt-T_8. The DNA structures to the left are theoretical models. The triplex structures in the center and on the right are average structures calculated from 400 molecular dynamics structures. (Graphics were generated using MidasPlus.) Reprinted with permission from ref 115. Copyright 2000 Adenine Press.

oligonucleotides. In these mixed-backbone oligonucleotides, the RNase H "inactive modifications" are placed at the 5′- and 3′-ends, while a central core of phosphodiester or phosphorothioate (PS) oligomers serves as a domain for RNase H activation. Mixed-backbone oligonucleotides have been reported to induce RNase H cleavage, increase stability against nucleases, and improve cellular uptake while potentially reducing adverse side effects.[121] In fact, several such chimeras are in clinical trials for the treatment of both solid tumors and AIDS.[122−125]

6.1. Incorporating Guanidinium and *S*-Methylthiourea Linkages into DNA[126,127]

The sequence nonspecific electrostatic attractive forces between DNA or RNA and DNG or DNmt could predominate over the complementary attraction of bases in extended sequences under physiological conditions. One way to decrease the electrostatic interactions would be to create mixed-backbone analogues—the strands would consist of mixed sequences of positive and negative linkers or positive and neutral linkers. Mixed-backbone nucleotides that incorporate guanidinium and *S*-Methylthiourea linkages into DNA (DNG/DNA or DNmt/DNA) have been prepared (Figure 16).

6.1.1. Synthesis. To facilitate the solid-phase synthesis of oligonucleotides that contain both DNA and DNG (or DNmt) monomers, building blocks **45** or **48** were prepared by condensing 2′-aminothimidine (**32**) with 3′-thiourea (**44**) or 3′-isothiocyanato (**47**) derivatives, respectively (Scheme 7). These monomers were then converted to the corresponding protected dimer phosphoramidites (**46**) or (**49**) and incorporated into oligonucleotides using standard solid-phase DNA synthesis in the 3′ → 5′ direction. The thiourea linkages in the oligonucleotides were methylated while on the solid support to give the *S*-Methylthiourea linkages.[127]

6.1.2. Thermal Denaturation Studies of DNG/DNA Chimeras[126]. Binding studies were conducted using DNG/DNA chimeras that contain either one, two, or three guanidinium linkages substituted in place of naturally occurring phosphodiester linkages (Figure 16). (The numerical prefix refers to the number of

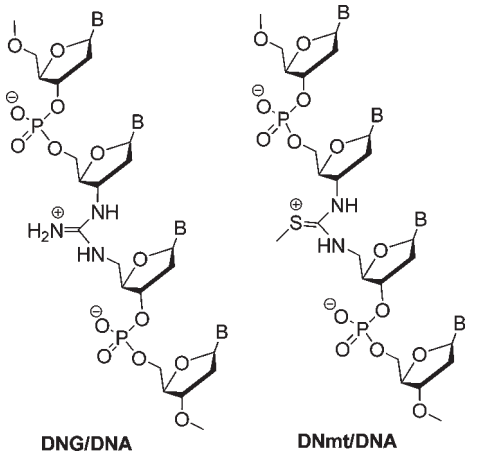

Figure 16. Structures of DNG/DNA and DNmt/DNA chimeras.

guanidinium substitutions; thus, 3DNG/DNA is a single-stranded chimera that contains three guanidinium substitutions.)

Each chimera was annealed to either fully cDNA (DNA-N_{18}^{comp}) or to DNA that contains a single mismatch (DNA-N_{18}^{mis}) (Figure 17). The buffer employed in these experiments contained 10 mM Na_2HPO_4 at pH 7.1. The oligomers form only antiparallel duplexes and lack the sequences necessary to form intra- or intermolecular complexes with themselves. A Job[128] plot confirmed that the binding stoichiometry of a (DNG/DNA) chimera with fully cDNA is 1:1. The stability of the duplexes was determined by thermal denaturation at three different salt concentrations in order to determine the effect of ionic strength on melting. The resulting melting points (T_m) are shown in Table 1.

In the absence of salt or at a low concentration (0.01 M), duplexes containing guanidinium linkages have a T_m identical (within experimental error) to that of native dsDNA (DNA-N_{18}·DNA-N_{18}^{comp}), as evidenced by the difference in the melting points of the chimeric and native duplexes ($\Delta T_m = T_m^{chimera} - T_m^{native}$) (Table 1). When the salt concentration is increased to 0.1 M, the duplex formed by the chimera with three guanidinium linkages (3DNG/DNA-N_{18}) shows a significant change in ΔT_m, indicating that the duplex has become less stable.

Because Na^+ screens the repulsive negative charges between the phosphate backbones, Na^+ stabilizes DNA·DNA interactions. In contrast, Na^+ interferes with the stabilizing interactions between the positively charged guanidinium groups of the chimera and the negatively charged phosphates of DNA.

The DNG/DNA chimeras, like the DNG oligomers, demonstrate sequence specificity. The stability of the duplexes formed between the chimeras (3DNG/DNA-N_{18}, 2DNG/DNA-N_{18}, and 1DNG/DNA-N_{18}) and DNA-N_{18} with a single mismatch (DNA-N_{18}^{mis}) was determined by thermal denaturation studies. Table 1 shows that the duplexes formed by all three chimeras with mismatched DNA are less stable than those formed by the same chimeras with fully cDNA. Using the T_m for DNA-N_{18}·DNA-N_{18}^{comp} as a reference, the ΔT_m's for the chimeras bound to DNA-N_{18}^{mis} were −11.0, −10.1, and −13.1 °C for one, two, and three guanidinium linkages, respectively. This decrease in melting temperature is similar to that observed for DNA-N_{18}·DNA-N_{18}^{mis} (ΔT_m = −9.1 °C).

6.1.3. Stability of DNG/DNA Chimeras Toward Exonuclease I[126]. Exonuclease I digests single-stranded DNA (ssDNA) by catalyzing the hydrolysis of the phosphodiester linkages in

Scheme 7[a]

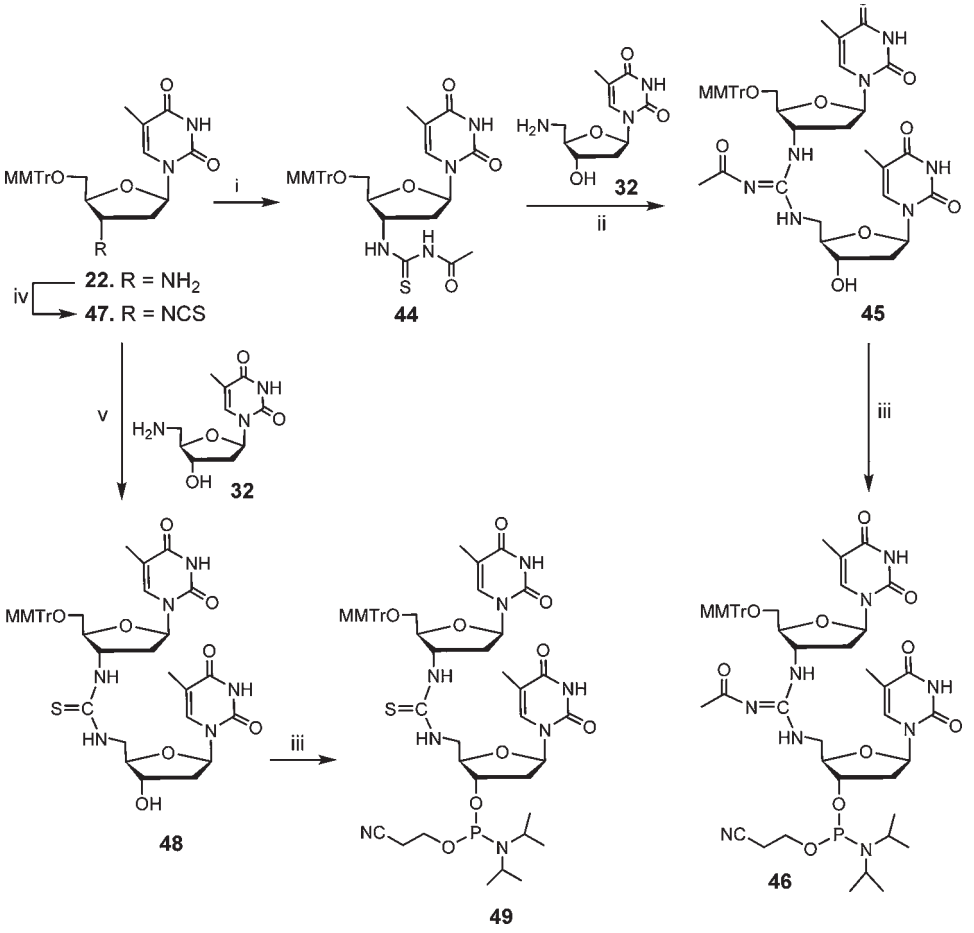

[a] (i) AcNCS, CH_2Cl_2, rt, 3 h; (ii) **32**, $HgCl_2$, TEA, rt, 12 h; (iii) $isoPr_2N(OCH_2CN)PCl$, $(isoPr_2CH)_2NH$, CH_2Cl_2, rt, 3 h; (iv) thiocarbonyl pyridone, CH_2Cl_2, rt, 6 h; (v) **32**, DMAP, pyridine, rt, 2 h.

3DNG/DNA-N_{18}	5′— d(**TgT**GTTAGT**TgT**TCTTG**TgT**T)
2DNG/DNA-N_{18}	5′— d(**TgT**GTTAGTTTTCTTG**TgT**T)
1DNG/DNA-N_{18}	5′— d(TTGTTAGT**TgT**TCTTGTTT)
DNA-N_{18}	5′— d(TTGTTAGTTTTCTTGTTT)
DNA-N_{18}^{comp}	5′— d(AAACAAGAAAACTAACAA)
DNA-N_{18}^{mis}	5′— d(AAACAAGA**T**AACTAACAA)

Figure 17. Location of the guanidinium substitutions in the DNG/DNA chimeras along with the position of the mismatch in the complementary sequence (**TgT** = guanidinium-linked thymidine dinucleotide in the chimeras; the DNA mismatch is underlined in bold).

Table 1. Melting Points for DNG/DNA Chimeras

	T_m (°C) at various [NaCl]		
duplex	0 M	0.01 M	0.1 M
DNA-N_{18}·DNA-N_{18}^{comp}	34.8	48.6	58.5
(3DNG/DNA-N_{18})·DNA-N_{18}^{comp}	34.8	46.6	53.5
(2DNG/DNA-N_{18})·DNA-N_{18}^{comp}	36.8	48.6	57.5
(1DNG/DNA-N_{18})·DNA-N_{18}^{comp}	34.8	47.6	56.5
DNA-N_{18}·DNA-N_{18}^{mis}		39.5	
(3DNG/DNA-N_{18})·DNA-N_{18}^{mis}		35.5	
(2DNG/DNA-N_{18})·DNA-N_{18}^{mis}		38.5	
(1DNG/DNA-N_{18})·DNA-N_{18}^{mis}		37.6	

the 3′ → 5′ direction [a process that can be followed by reversed phase high pressure liquid chromotography (RP-HPLC)]. Thus, a chimera capped with a guanidinium linkage at the 3′-end would be expected to be resistant to hydrolysis by exonuclease I. Both 3DNG/DNA-N_{18} and 2DNG/DNA-N_{18} (Figure 17) have guanidinium linkages at the 3′-end and are completely resistant toward hydrolysis even after 12 h of incubation. 1DNG/DNA-N_{18}, with a guanidinium linkage at its center, was found to be only partially hydrolyzed after 1 h, with no further hydrolysis after 12 h. Thus, guanidinium linkages placed at the ends of a chimera confer complete resistance to exonuclease I. Furthermore, the partial hydrolysis of 1DNG/DNA-N_{18} indicates that phosphodiester linkages around the guanidinium are stable to cleavage.

6.1.4. Thermal Denaturation Studies of DNmt/DNA Chimeras[127]**.** Three chimeras, containing either one or two positively charged *S*-methylthiourea linkages in place of phosphodiester linkages, were examined for their ability to form stable duplexes with both complementary and mismatched DNA. The structures of the chimeras are shown in Figure 18. The duplexes formed by 1DNmt/DNA-T_{15} or 2DNmt/DNA-T_{15} chimeras

dx.doi.org/10.1021/cr1004265 |*Chem. Rev.* 2012, 112, 1284–1309

2DNmt/DNA-T_{15}	5′–d(T**T_{mt}**TTTTTTTTT**T_{mt}**TT)
1DNmt/DNA-T_{15}	5′–d(TTTTTT**T_{mt}**TTTTTTT)
2DNmt/DNA-N_{18}	5′–d(**T_{mt}**TGTTAGTTTTCTTG**T_{mt}**TT)
DNA-N_{18}	5′–d(TTGTTAGTTTTCTTGTTT)
DNA-N_{18}^{comp}	5′–d(AAACAAGAAAACTAACAA)
DNA-T_{15}	5′–d(TTTTTTTTTTTTTTT)
DNA-A_{15}	5′–d(AAAAAAAAAAAAAAA)
DNA-A_{15}^{mis1}	5′–d(AAAAAAAAAAAA**T**AA)
DNA-A_{15}^{mis2}	5′–d(AA**T**AAAAAAAAAAA)
DNA-A_{15}^{mis3}	5′–d(AAAAAA**T**AAAAAAAA)

Figure 18. Sequences of DNA and DNmt/DNA chimeras (**Tmt** = *S*-methylthiourea-linked thymidine nucleotide in the chimeras; DNA mismatches are underlined in bold).

Table 2. Melting Temperatures for (DNmt/DNA)·DNA Duplexes

	T_m (°C) at various [NaCl]		
duplex	0 M	0.01 M	0.1 M
DNA-T_{15}·DNA-A_{15}	19.8	23.6	33.4
(2DNmt/DNA-T_{15})·DNA-A_{15}	17.6	20.3	30.0
(1DNmt/DNA-T_{15})·DNA-A_{15}	17.8	20.2	29.9
DNA-N_{18}·DNA-N_{18}^{comp}	31.7	36.0	47.0
(2DNmt/DNA-N_{18})·DNA-N_{18}^{comp}	32.1	36.1	46.1

with DNA-A_{15} have essentially identical sets of melting points (T_m) that increase with increasing ionic strength (Table 2).

Each of the chimeras forms a duplex in a 1:1 ratio with ssDNA. The CD spectra of all the (DNmt/DNA)·DNA duplexes are similar to that reported for dT_{19}·dA_{19}, confirming that the chimeras form double-helical structures with DNA. Thermal denaturation studies produced sigmoidal temperature vs absorbance curves, indicating that double helix formation is cooperative.

In the absence of salt, the (2DNmt/DNA-T_{15})·DNA-A_{15} duplex has a ΔT_m = −2.2 °C compared to that of the native DNA-T_{15}·DNA-A_{15} duplex. This small destabilization increases slightly (ΔT_m = −3.3 °C) in 0.01 M NaCl, and no additional change is observed (ΔT_m = −3.4 °C) in 0.1 M NaCl. In the case of the mixed-base duplex, (2DNmt/DNA-N_{18})·(DNA-N_{18}^{comp}), the T_m is essentially identical to that of the native (DNA-N_{18}·DNA-N_{18}^{comp}) duplex, even at the highest salt concentration. Thus, incorporation of *S*-methylthiourea linkages into DNA has little, if any, effect on the electrostatics of duplex formation.

To determine whether *S*-methylthiourea linkages display sequence specificity, the chimeras were complexed to ssDNA containing a single mismatch at the 3′-end, at the 5′-end, or at the center (Figure 18). The centrally placed mismatch (DNA-A_{15}^{mis3}) causes maximum destabilization in both the (DNmt/DNA)·(DNA) and DNA·DNA duplexes (third column of Table 3). Furthermore, 3′-end mismatches are better tolerated than 5′-end mismatches in all cases. Because (DNmt/DNA) chimeras are sensitive to mismatches, we can conclude that they display sequence specificity.

Table 3. Melting Temperatures for (DNmt/DNA)·DNA Mismatched Duplexes at [NaCl] = 100 mM

	T_m (°C) for X·Y mismatched duplexes			
X/Y	DNA-A_{15}	DNA-A_{15}^{mis1}	DNA-A_{15}^{mis2}	DNA-A_{15}^{mis3}
DNA-T_{15}	33.4	28.7	30.0	24.2
2DNmt/DNA-T_{15}	30.0	26.5	28.5	19.8
1DNmt/DNA-T_{15}	29.9	24.4	26.2	22.2

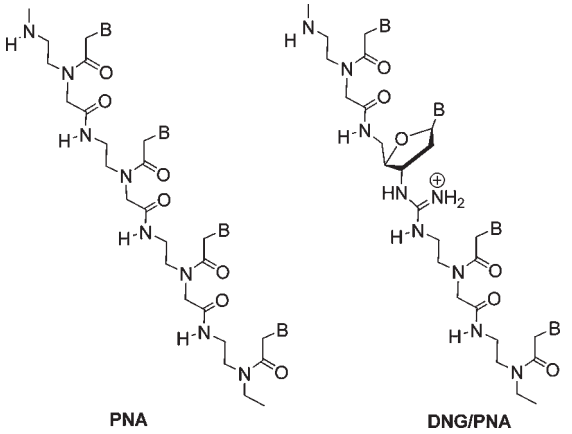

Figure 19. Structures of PNA and mixed-backbone PNA/DNG oligonucleotides.

6.1.5. Stability of DNmt/DNA Chimeras Toward Exonuclease I[127]. The three DNmt/DNA chimeras, along with the DNA-T_{15} control, were subjected to cleavage by exonuclease I, and the products analyzed by RP-HPLC. DNA-T_{15} was readily hydrolyzed within 1 h of incubation. The two chimeras with *S*-methylthiourea linkages at both the 3′- and 5′-ends, 2DNmt/DNA-T_{15} and 2DNmt/DNA-N_{18} (Figure 18), were not hydrolyzed even after 12 h. The chimera with one centrally placed *S*-methylthiourea linkage, 1DNmt/DNA-T_{15} (Figure 18), was partially hydrolyzed after 1 h and no further hydrolysis occurred after 12 h. Because the enzyme hydrolyzes phosphodiester linkages in the 3′ → 5′ direction, it is not surprising that chimeras with *S*-methylthiourea linkages at the 3′-end are completely resistant to hydrolysis.

6.2. Incorporating DNG Linkages into PNA[129,130]

The linkages in peptide nucleic acids (PNAs) are not charged (Figure 19). A favorable conformational structure and lack of electrostatic repulsion result in a high binding affinity of PNA for its DNA or RNA targets.[131] However, PNAs have serious limitations for therapeutic applications because of their poor solubility and poor cell membrane permeability.[132,133] Studies with PNAs have been performed in vitro[134] by employing microinjection[135] and carrier peptides.[136]

Guanidinium linkages were used to introduce positive charges into a PNA sequence (Figure 20), anticipating that the positive charges would provide greater solubility and enhanced cell-membrane permeability, would inhibit self-aggregation of PNA, and would increase the equilibrium and rate constants for association with DNA or RNA.

6.2.1. Synthesis. The solid-phase synthesis of PNA and DNG/PNA chimeras (**I**−**IV**) was carried out using monomer

56[137] for the synthesis of PNA and building block **55** for the incorporation of DNG/PNA dimeric units into PNA. The guanidinium-linked dimer (**55**) was obtained by condensing the carbodiimide (**53**), generated in situ from the corresponding thiourea (**52**) and 3′-aminothymidine derivatives (**25**) (Scheme 8).[129,130]

6.2.2. Thermal Denaturation Studies of DNG/PNA Chimeras[129,130]**.** Four (DNG/PNA) chimeras were synthesized that differed in the number and location of the guanidinium linkages: (i) a centrally placed guanidinium linkage; (ii) two guanidinium linkages, one placed at each terminus; (iii) two centrally placed guanidinium linkages; (iv) three guanidinium linkages, one at the center and one at each terminus (Figure 20). The "**t**" in Figure 20 indicates a thymidine base linked to a PNA backbone, and "**Tg**" indicates a thymidine base with a 3′-guanidinium linkage. All of the chimeras and one of the PNA oligomers (PNA-A_{10}) possess hydroxyhexylamide (R = $NH(CH_2)_6OH$) at the C-terminus. A second PNA oligomer (PNA-A_{10}^{lys}) possesses a positively charged lysine at the C-terminus. The targets for the DNG/PNA and PNA oligomers were non-self-complementary, length-matched, ssDNA oligonucleotides. Job plots (Figure 21) show that the binding stoichiometry of PNA or DNG/PNA chimeras to complementary ssDNA is 2:1, indicating the formation of $(PNA)_2$·DNA or $(DNG/PNA)_2$·DNA triplexes. Circular dichroism studies also indicate that $(PNA)_2$·DNA and $(DNG/PNA)_2$·DNA have similar triple helical structures.[130]

1DNG/PNA-T_{10}	H_3N^+–t t t t **Tg** t t t t t–R
e2DNG/PNA-T_{10}	H_3N^+–**Tg** t t t t t t t **Tg** t–R
c2DNG/PNA-T_{10}	H_3N^+–t t t **Tg** t **Tg** t t t t–R
3DNG/PNA-T_{10}	H_3N^+–**Tg** t t t **Tg** t t t **Tg** t–R
PNA-T_{10}	H_3N^+–t t t t t t t t t t–R
PNA-T_{10}^{lys}	H_3N^+–t t t t t t t t t t–Lys^+
DNA-A_{10}	5′–d(AAAAAAAAAA)–3′
DNA-A_{10}^{mis}	5′–d(AAAA**G**AAAAA)–3′

Figure 20. The sequences of DNA, PNA, and DNG/PNA chimeras used to determine the triplex melting points in Table 4 (R = −NH−$(CH_2)_6$−OH, *t* = thymidine PNA nucleotide, **Tg** = thymidine DNG nucleotide; the DNA mismatch is underlined in bold).

Thermal denaturation studies were used to determine the stability of $(PNA)_2$·DNA and $(DNG/PNA)_2$·DNA triplexes. Curve fitting and first-derivative analysis of the melting curves (Figure 22) locate the inflections and corresponding melting points (T_m) shown in Table 4. Because PNA-T_{10} (Figure 20) does not have a positively charged lysine at the C-terminus, the $(PNA\text{-}T_{10})_2$·DNA-A_{10} triplex has a lower T_m (54.5 °C) than that reported for $(PNA\text{-}T_{10}^{lys})_2$·DNA-$A_{10}$ (T_m = 72.0 °C).[131] DNG/PNA chimeras that contain internal guanidinium linkages show a marked destabilization that may be due to unfavorable structural changes in their backbones. The e2DNG/PNA-A_{10} chimera, with a guanidinium linkage at each terminus, forms a triplex with a T_m = 52.5 °C, close to that of the nonchimeric $(PNA\text{-}T_{10})_2$·DNA-A_{10} triplex (T_m = 52.5 °C).

To assess the sequence specificity of the DNG/PNA chimeras, the sequences were hybridized to complementary ssDNA containing one central mismatched base (A → G). Triplexes $(PNA\text{-}T_{10})_2$·DNA-A^{mis} and $(e2DNG/PNA\text{-}T_{10})_2$·DNA-$A^{mis}$ exhibit a 16 and 13 °C decrease in T_m, respectively, compared to the T_m of the fully complementary triplexes (Table 4). Destabilization due to a single mismatch indicates that the binding of chimera (e2DNA/PNA-T_{10}) to DNA-A_{10} is sequence specific and involves both Watson−Crick and Hoogsteen hydrogen bonding. Note that all the triplexes in Table 4, including the mismatches,

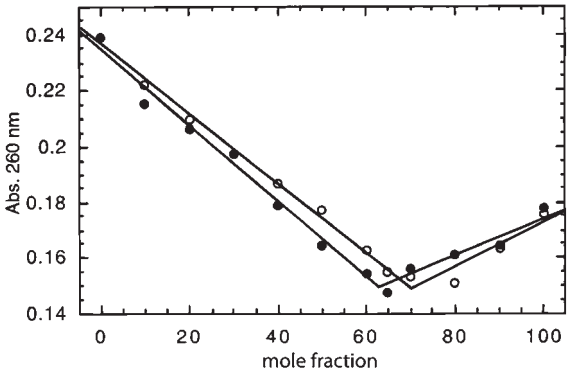

Figure 21. 2:1 stoichiometry for triplex hybridization. (●) = $(e2DNG/PNA\text{-}T_{10})_2$·DNA-$A_{10}$ and (○) = $(PNA\text{-}T_{10})_2$·DNA-A_{10}. Reprinted with permission from ref 130. Copyright 2000 American Chemical Society.

Scheme 8[a]

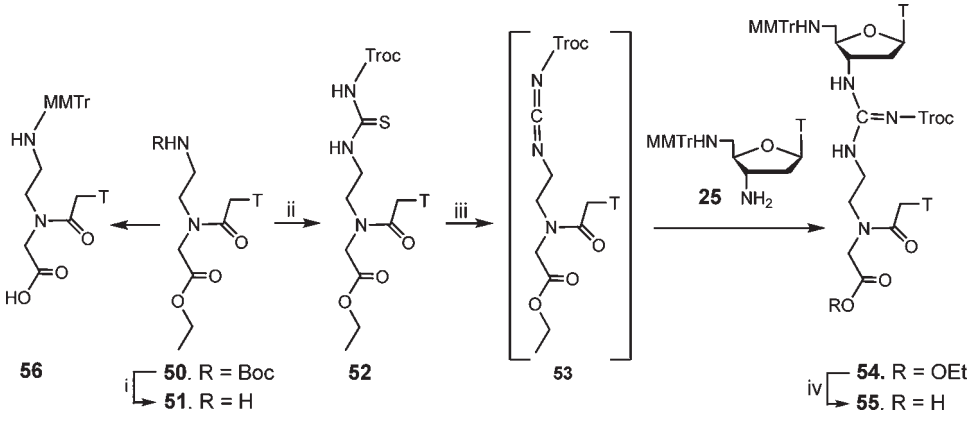

[a] (i) Trifluoroacetic acid, (ii) $Cl_3CCH_2(C{=}O)ONCS$, TEA, CH_2Cl_2; (iii) $HgCl_2$, DIPEA, DMF; (iv) NaOH, dioxane/water.

dx.doi.org/10.1021/cr1004265 |*Chem. Rev.* 2012, 112, 1284–1309

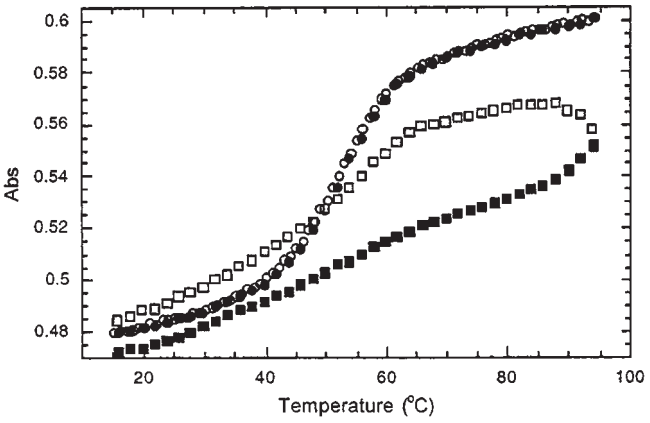

Figure 22. Melting and annealing curves. (●) = (e2DNG/PNA-T_{10})$_2$·DNA-A_{10} melting; (○) = (e2DNG/PNA-T_{10})$_2$·DNA-A_{10} annealing; (■) = (PNA)$_2$·DNA-A_{10} melting; (□) = (PNA)$_2$·DNA-A_{10} annealing. Reprinted with permission from ref 130. Copyright 2000 American Chemical Society.

have T_m's greater than that observed for the corresponding DNA triplex (dT_{10})$_2$·dA_{10} ($T_m \sim 10$ °C).

The shapes of the melting curves in Figure 22 are of particular interest. The percentage of hypochromicity that accompanies the formation of the (e2DNG/PNA-T_{10})$_2$·DNA-A_{10} triplex (25.4%) exceeds that of the (PNA-T_{10})$_2$·DNA-A_{10} triplex (17.8%), indicating that there is better base stacking in the chimeric triplex. In thermal denaturation studies, hysteresis is observed between heating and cooling curves, because the rate of association between oligomers to form a duplex or triplex is slower than the rate of dissociation. The most significant result is that the (e2DNG/PNA-T_{10})$_2$·DNA-A_{10} triplex shows no hysteresis upon cooling (that is, the melting and annealing curves overlap). Thus, the on/off rates are nearly equivalent for hybridization of e2DNG/PNA-T_{10} with cDNA-A_{10}. The sequence specificity and the increased rate of association suggest a possible use of DNG/PNA chimeras in diagnostics, biomolecular probes, and antisense/antigene therapeutics.

6.2.3. Gel Shift, Strand Invasion, and Binding Kinetics[130]. The binding properties of the e2DNG/PNA-T_{10} chimera (Figure 20) and PNA-T_{10}^{lys} with an 80-base-pair (bp) dsDNA ^{32}P-radioactively labeled at a 5′-end were studied under physiological, isothermal conditions (37 °C). The 80-bp dsDNA contained the DNA-A_{10} target sequence, as well as sites with one (5′-dA_4TA_5) and three (5′-dATA_2TA_2TA_2) base mismatches.

5′-GACCCGTGCGGATCC**A_4TA$_5$**CGTGGCTGCG**A_{10}**GTCGTGCTCCATA**$_2$TA$_2$TA$_2$**GCTTC GCTCCAGGTC-3′

3′-CTGGGCACGCCTAGG**T_4AT$_5$**GCACCGACGC**T_{10}**CAGCACGAGGTA**T_2AT$_2$AT$_2$**CGAA GCGAGGTCCAG-5′

80 base pair dsDNA

Although the thermal stability of triplexes (e2DNG/PNA-T_{10})$_2$·DNA-A_{10} and (PNA-T_{10})$_2$·DNA-A_{10} are similar, gel shift assays under isothermal conditions show that the e2DNG/PNA-T_{10} chimera binds dsDNA more favorably than does PNA-T_{10}. In the gel shift assay, different concentrations (0, 0.1, 0.5, and 2.0 μM) of the chimeric and PNA oligomers are mixed with dsDNA (0.005 μM) and then analyzed by electrophoresis on a nondenaturing polyacrylamide gel. Because of increased mass, the complexes between the chimera or PNA with dsDNA migrate a shorter distance along the gel than does the 80-bp dsDNA alone. At a concentration of 2 μM, the e2DNG/PNA-T_{10} chimera shows a dark band on the gel corresponding to binding to the 80-bp dsDNA. In contrast, even at a concentration of 2 μM, very little binding of PNA-T_{10} to the 80-bp dsDNA is evident on the gel.[130]

Table 4. Melting Points of the Triplexes

triplex	T_m (°C)
(PNA-T_{10})$_2$·DNA-A_{10}	54.5
(1DNG/PNA-T_{10})$_2$·DNA-A_{10}	29.5
(e2DNG/PNA-T_{10})$_2$·DNA-A_{10}	52.5
(c2DNG/PNA-T_{10})$_2$·DNA-A_{10}	25.5
(3DNG/PNA-T_{10})$_2$·DNA-A_{10}	25.5
(PNA-T_{10})$_2$·DNA-A^{mis}	38.5
(e2DNG/PNA-T_{10})$_2$·DNA-A^{mis}	39.5

Figure 23. Strand invasion of dsDNA by a PNA/DNG chimera forms a triplex and creates a D-loop.

S1 nuclease cleavage protection assays were performed to determine whether e2DNG/PNA-T_{10} binds dsDNA by triplex formation (e2DNG/PNA-T_{10})·(DNA)$_2$ or by strand invasion of dsDNA resulting in (e2DNG/PNA-T_{10})$_2$·(DNA) with an accompanying D-loop (Figure 23). After the chimeric and PNA oligomers were incubated (separately) with 80-bp dsDNA at 37 °C, the mixtures were subjected to S1 digestion and then separated by electrophoresis on a denaturing polyacylamide gel. Analyses indicate that both the e2DNG/PNA-T_{10} strand and the PNA-T_{10}^{lys} strand invade dsDNA, displacing the nonsequence cDNA single strand (T_{10}), which then becomes a substrate for S1 nuclease cleavage (Figure 23).

To determine the kinetics of binding, the 80-bp dsDNA was incubated with the chimera and (separately) with PNA for different periods of time, and then separated by gel electrophoresis. Quantification of the bands shows that e2DNG/PNA-T_{10} associates with 80-bp dsDNA at a greater rate (30 min; 75%) than does PNA-T_{10}^{lys} (30 min; 58%). This is in agreement with the on/off rates observed in the thermal denaturation studies (Figure 22).

7. DNG WITH A TETHERED HOECHST 33258 FLUOROPHORE[138]

It is well documented that covalent binding of intercalators,[139] polyamines,[140] or fluorescent dyes[141−143] to oligonucleotides can enhance the stability of duplexes and triplexes.[144−148] Among these ligands, the Hoechst 33258 dye is the best known. It binds in the minor groove with a strong preference for A·T base pairs. Binding in the minor groove greatly enhances the fluorescence of the dye.[149−153] Hoechst 33258 is capable of crossing cellular and nuclear membranes.[154−156]

To further enhance the already strong binding of a DNG to cDNA, DNG-Hoechst conjugates (DNG-T_5-Ho, **66**, and **67**) were prepared in which a Hoechst dye is tethered to the 5′-end of DNG-T_5 (Scheme 9). The DNG-T_5-Ho conjugates bind

Scheme 9[a]

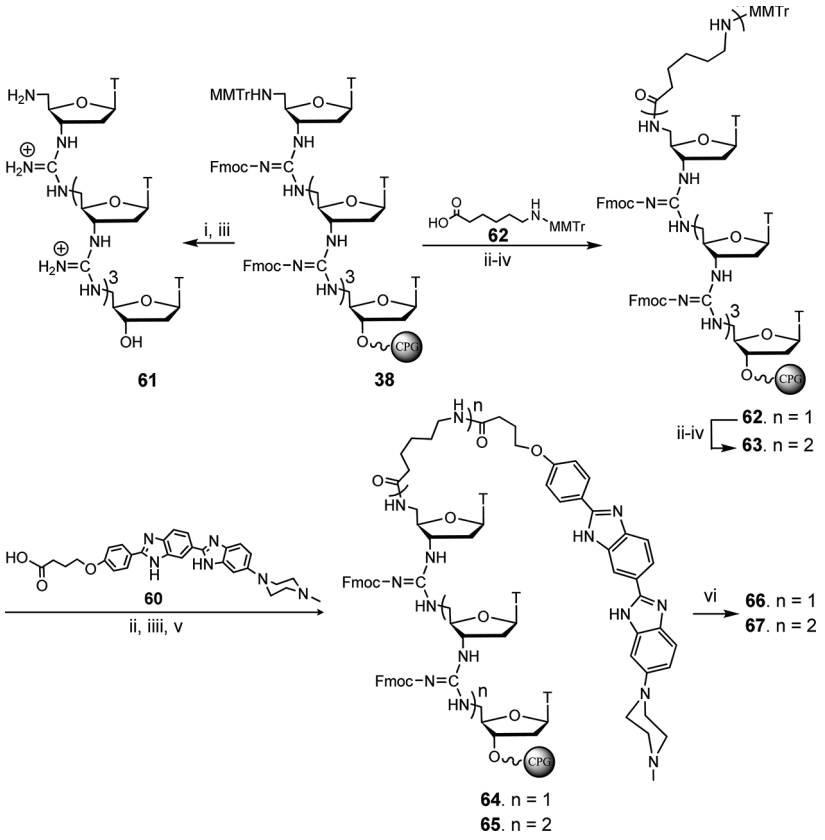

[a] (i) Methanolic ammonia, rt, 2 h. (ii) Capping: Ac_2O, TEA, DMF, 10 min. (iii) Deprotection: 3% dichloroaetic acid in CH_2Cl_2, 1 min. (iv) Coupling: monomer **62**, PyBOP, HOBt, DIPEA, DMF, 12 h; (v) Ht acid **60**, PyBOP, HOBt, DIPEA, DMF, 24 h. (vi) 0.1 M NaOH in 4:1 MeOH/H_2O, 1 h. Ht = Hoechst 33258.

sequence specifically to the A·T target site of dsDNA to form a dsDNA(A-T)·DNG-T_5-Ho triplex in which the DNG-T_5 strand is located in the major groove and the Hoechst ligand occupies the minor groove. Similarly, DNG-T_5-Ho forms a stable ssDNA-A_5·DNG-T_5-Ho duplex by binding sequence specifically to the A-rich target site of ssDNA (Figure 24).

7.1. Synthesis[138]

To obtain DNG-Hoechst conjugates with different linker lengths, building blocks **60** and **62** were prepared. The Hoechst acid (**60**) was prepared by condensing the benzaldehyde derivative (**57**) with an ortho-diamine (**58**),[157] followed by hydrolysis of the ester (Scheme 10); tritylation of commercially available 6-aminohexanoic acid gave building block **62** (Scheme 10).

DNG-T_5 (**38**) was synthesized on a solid support in the 3′ → 5′ direction (Scheme 5), similar to DNA solid-phase synthesis. The DNG-Hoechst conjugates (**64**) and (**65**) with 11- and 18-atom linkers, respectively, were prepared by addition of the linker building blocks (**62** and **60**) to the 5′-end of DNG-T_5 (**38**) using PyBOP/HOBt chemistry. For a control study, DNG-T_5 (**61**) was also prepared from **38** (Scheme 9).

7.2. Binding and Thermal Denaturation Studies of dsDNA·DNG-Hoechst Triplexes[138]

A comparative study of the stabilities of the triplexes formed by both DNG-T_5 (**61**) and DNG-T_5-Ho conjugates (**66** or **67**) with a 30-mer dsDNA duplex containing a pentameric AAAAA/TTTTT tract at the center as the target site (Figure 25) was carried out.

The triplexes formed with the Hoechst-tethered conjugates are significantly more stable (ΔT_m +14 °C) than the triplex formed with DNG-T_5. The greater stability of the former is due to simultaneous binding to both the major and minor grooves of the dsDNA target site. Changing the length of the tether from 18- to 11-atoms does not affect the triplex T_m significantly, which indicates that the 11-atom linker is long enough to traverse the backbone, permitting the Hoechst ligand to reside deep in the A·T rich minor groove. As expected, an increase in ionic strength significantly decreases the T_m values of the triplexes.

Incorporation of a G·C mismatched pair in the center of the dsDNA target site (AAGAA/TTCTT) results in a dramatic decrease in both the stability of the dsDNA·DNG-T_5 triplex (from T_m = 36 °C to T_m = 25 °C) and the stabilities of the dsDNA·DNG-T_5-Ho triplexes (**66** and **67**) (from T_m = 49 °C to T_m = 26 °C). Thus, binding the DNG-T_5-Ho conjugates to dsDNA is highly sequence specific. With two G·C base pair mismatches (AGAGA/TCTCT), triplex formation does not occur.

Inversion of an A·T base pair to T·A base pair in the center of the target site (AATAA/TTATT) decreases the stability of the dsDNA·DNG-T_5 triplex to the same extent as is found with the G·C mismatched pair (from T_m = 36 °C to T_m = 25 °C), but only a slight decrease in stability is observed in the case of the dsDNA·DNG-T_5-Ho triplexes (from T_m = 49 °C to T_m = 44 °C). Thus, the tethered Hoechst moiety is still able to bind tightly in the T·A rich minor groove.

dx.doi.org/10.1021/cr1004265 |*Chem. Rev.* 2012, 112, 1284–1309

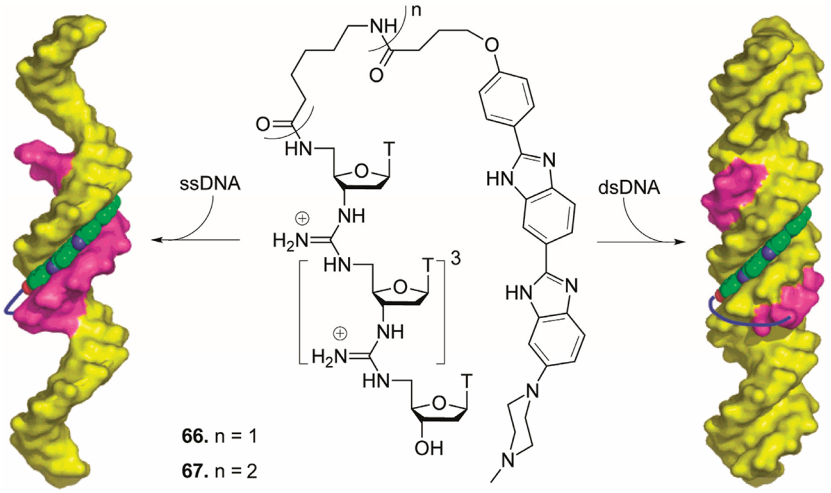

Figure 24. Models of a DNA·DNG-Ho duplex and a dsDNA·DNG-Ho triplex formed by DNA and DNG−Hoechst 33258 conjugates. ssDNA and dsDNA are yellow, DNG is magenta, the Hoechst dye is green, and the linker is blue.

Scheme 10[a]

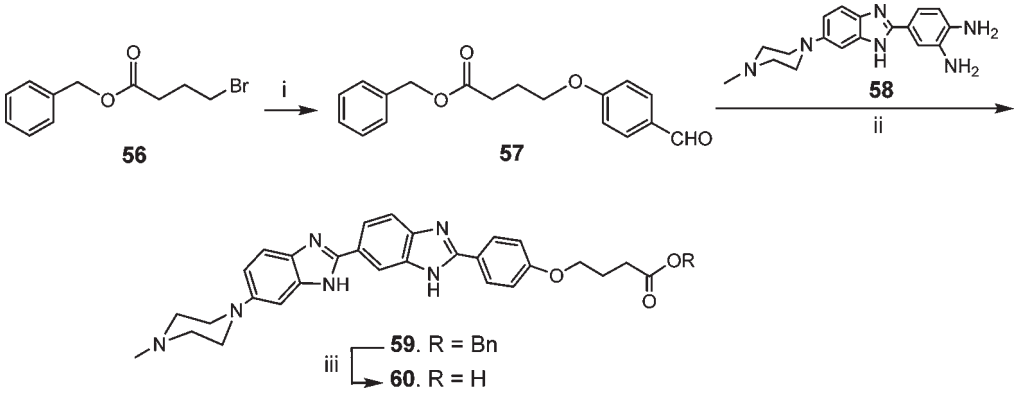

[a] (i) 4-Hydroxybenzaldehyde, Cs_2CO_3, anhydrous DMA, 100 °C, 15 h; (ii) nitrobenzene, 130 °C 24 h; (iii) 10% Pd/C, H_2, EtOH, 4 h.

Figure 25. Triplexes formed by a 30-mer dsDNA and DNG-T_5−(aliphatic tether)−Ho conjugates (X = T; Y = A).

7.3. Fluorescence Characteristics of a dsDNA·DNG-Hoechst Triplex

When target dsDNA binds the DNG-Ho conjugates (**66** and **67**), a strong fluorescence emission at 450 nm is observed. dsDNA/Hoechst 33258 complexes emit a similar signal at 445 nm. The fluorescence emission decreases significantly when G·C mismatches are introduced at the center of the binding site (AAGAA/TTCTT), indicating that the Hoechst fluorophore can no longer bind. However, the triplex formed with a T·A mismatch (AATAA/TTATT) exhibits fluorescence enhancement similar to the triplex formed with a nonmismatched sequence. This observation supports the assertion that the complexation of DNG-T_5-Ho with the dsDNA target site results in formation of a local dsDNA·DNG-T_5-Ho triplex in which the DNG strand occupies the major groove and the Hoechst ligand binds simultaneously in the minor groove (Figure 24).

7.4. Binding and Thermal Denaturation Studies of DNA·DNG-T_5-Hoechst Duplexes

The thermal melting studies of duplexes formed by DNG-T_5-Ho conjugates (**66** and **67**) with DNA-A_5 indicate a ΔT_m of +2 °C compared to a DNG-T_5·DNA-A_5 duplex. Thus, the Ho moiety of **66** and **67** has little influence on the stability of DNG-T_5·DNA-A_5. However, binding **66** and **67** to a 30-mer ssDNA with a pentameric adenyl binding site in the middle of the sequence (CGCCGCGC-GCGCG**AAAAA**CCGGCGCGCGC) shows a ΔT_m of +7 °C compared to that of the duplex formed by DNG-T_5 (**61**) (lacking the Hoechst ligand) with 30-mer ssDNA. This increase in T_m when compared with that of the 30-mer dsDNA·DNG-T_5-Ho triplex (ΔT_m = +13 °C) indicates that the Hoechst ligand is very weakly bound, which may be due to a narrowing of the minor groove of the DNA·DNG duplex or to a positive charge−charge repulsive effect of the DNG backbone and the piperazine ring of the Hoechst ligand.

Binding of conjugates **66** and **67** to ssDNA is highly sequence specific. Incorporation of a single C mismatch in the central binding site of the 30-mer DNA sequence results in a significant decrease in the T_m value compared to that for DNA without a mismatch. The effect is more pronounced with an internal mismatch (AA**C**AA, ΔT_m = −8 °C) than with 5′- or 3′-terminal mismatches (**C**AAAA or AAAA**C**, ΔT_m = −5 °C).

dx.doi.org/10.1021/cr1004265 |*Chem. Rev.* 2012, 112, 1284–1309

7.5. Fluorescence Characteristics of DNA·DNG-T5-Hoechst Duplexes

A weak fluorescence signal is obtained when conjugates **66** and **67** complex with complementary pentameric adenyl ssDNA.

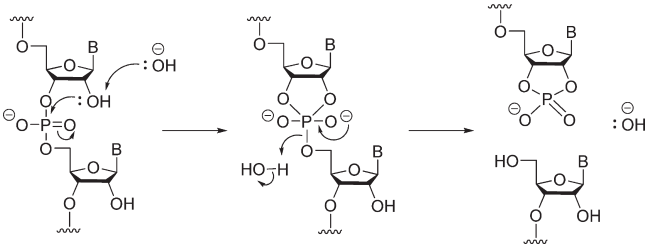

Figure 26. Intramolecular splicing of RNA.

This suggest that the Hoechst dye cannot bind effectively in the minor groove of the DNA-A_5·DNG-T_5 duplex. However, the fluorescence emission signal increases significantly when **66** and **67** bind to a 30-mer ssDNA with a pentameric adenyl binding site in the middle (CGCCGCGCGCGCG**AAAAA**CCCGGCGC-GCGC). The presence of long G·C sequences on either side of the target adenyl site provides a flexible DNA·DNG minor groove in which the tethered Hoechst dye can bind (Figure 24).

8. OLIGORIBONUCLEOTIDES WITH GUANIDINIUM BACKBONES (RNGS)[158−162]

Replacing the negatively charged phosphodiester linkages of RNA with positively charged guanidinium linkages provides polycationic ribonucleic guanidine (RNG). RNGs are stable to

Scheme 11[a]

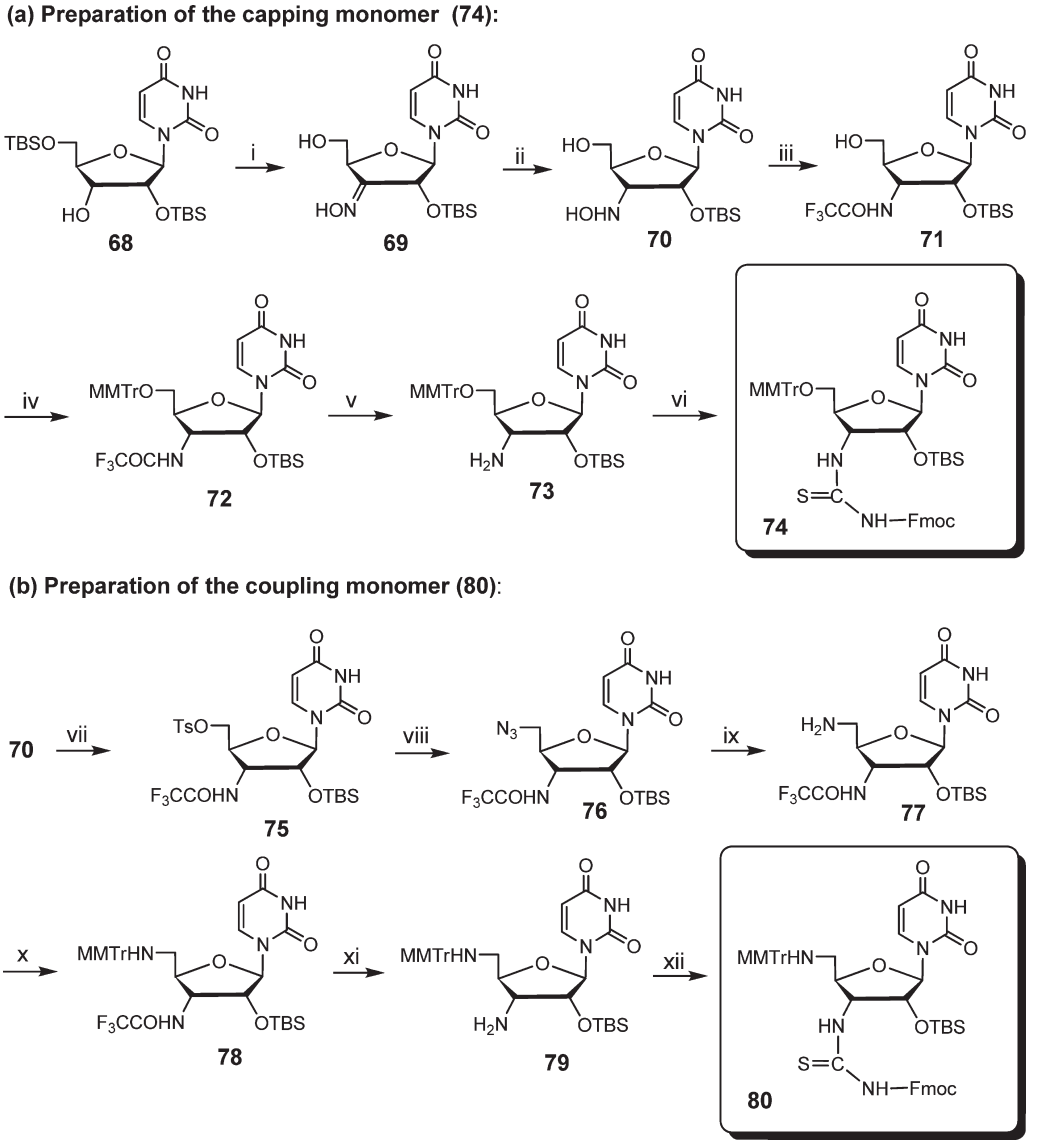

[a] Reagents and conditions: (i) (a) CrO_3, pyridine, Ac_2O, 4 Å molecular sieves, CH_2Cl_2, 0 °C, (b) NH_3OHCl, pyridine, rt; (ii) $NaBH_4$, AcOH, 5 °C; (iii) (a) H_2, 10% Pd/C, 90% Aq. AcOH, rt, (b) CF_3COOEt, Et_3N, MeOH, rt, (iv) (a) MMTrCl, pyridine, rt, (b) NH_3/MeOH, rt; (vi) Fmoc-NCS, CH_2Cl_2, rt; (vii) TsCl, pyridine, rt; (viii) NaN_3 ; NH_4Cl, DMF, 80 °C (ix) (a) H_2S (g), 60% aq. pyridine, rt; (x) MMTrCl, pyridine, rt; (xi) NH_3/MeOH, rt; (xii) Fmoc-NCS, CH_2Cl_2, rt.

dx.doi.org/10.1021/cr1004265 |*Chem. Rev.* 2012, 112, 1284–1309

Scheme 12[a]

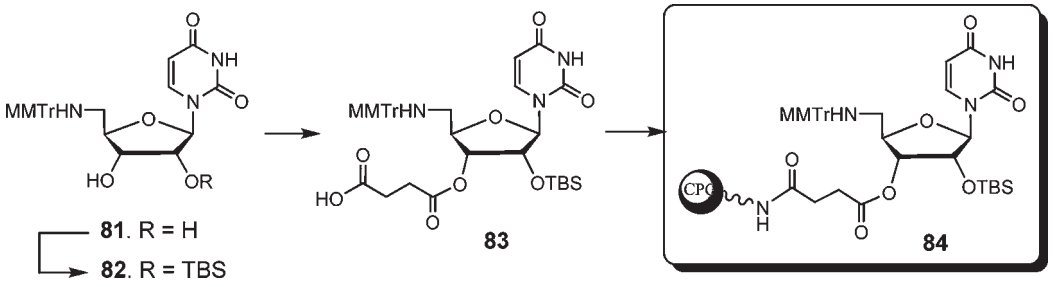

[a] Reagents and conditions: (i) TBSCl, $AgNO_3$, pyridine, THF, rt; (ii) succinic anhydride, DMAP, pyridine, rt; (iii) LCAA-CPG, 1-(3-dimethylaminopropyl)-3-ethylcarbodiimide hydrochloride, DMF, rt.

Scheme 13. Solid-Phase Synthesis[a]

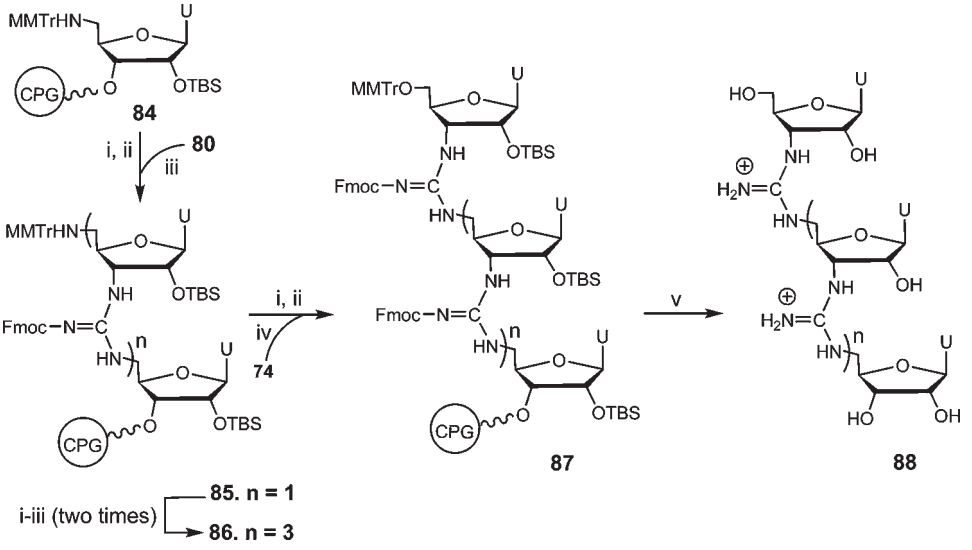

[a] Reagents and conditions: (i) capping: (1) CF_3COOEt, DIEA, DMF; (ii) deblocking: 3% dichloroacteic acid in CH_2Cl_2; (iii) coupling: (1) **80**, $HgCl_2$, DIEA, DMF, (2) 20%, thiophenol in DMF; (iv) coupling of the 5′-terminal monomer: (1) **74**, $HgCl_2$, DIEA, DMF; (2) 20% thiophenol in DMF; (v) cleavage and deprotection: (1) 3% dichloroacteic acid in CH_2Cl_2, (2) NH_4OH/EtOH; (3) 1.0 M TBAF in THF.

both nuclease degradation and to intramolecular nucleophilic attack by the C-2′-OH (Figure 26) group and are therefore better suited than RNA to be antisense/antigene agents (Figure 6).

8.1. Synthesis[159,160]

The monomers (**74** and **80**) required for solid-phase synthesis of uridyl RNG were prepared from 2′,5′-disilyluridine via a 3′-deoxy-3′-(hydroxylamino)-uridine derivative (**70**) (Scheme 11).

The 3′-terminal building block (**83**) was prepared from the 5′-tritylaminouridine derivative (**81**) and was attached to the solid support as described in Scheme 12. The solid-phase synthesis of RNG-U_5 was carried out by removing the MMTr protecting group of **84** and coupling with in situ generated carbodiimide from monomer **80** or **74** in the presence of $HgCl_2/Et_3N$, as was described for DNG (Scheme 13).

8.2. Binding and Thermal Denaturation Studies[161,162]

Job plots of an aqueous solution of RNG-U_5, DNA-A_5, and RNA-A_5 show the formation of RNG-U_5·DNA-A_5 and RNG-U_5·RNA-A_5 duplexes. Thermal melting studies show that RNG-U_5 binds with unprecedented affinity to DNA-A_5. The T_m value for RNG-U_5·DNA-A_5 is 62 °C; in contrast, the extrapolated T_m values for RNA-U_5·DNA-A_5 and DNA-T_5·DNA-A_5 are 0 and −10 °C, respectively. Thus, RNG, while maintaining base-pair specificity, exhibits a much greater affinity for DNA than does RNA.

Introducing a one-base mismatch in the DNA component (RNG-U_5·AAAAT) decreases the T_m value of the duplex from 62 to 55 °C; DNA with two or three mismatches (ATATA, TATAT) shows no interaction with RNG-U_5.[161]

Thermodynamic calculations[161] reveal that RNG·DNA duplex formation (pH 7; $\mu = 0.12$) is over 1000 times more favorable than RNA·DNA or RNA·RNA duplex formation. In contrast, the RNG-U_5·RNA-A_5 duplex is much less stable. The order of thermal stability is RNG-U_5·DNA-A_5 > RNA-U_5·RNA-A_5 > RNG-U_5·RNA-A_5 > RNA-U_5·DNA-A_5 > DNA-T_5·DNA-A_5.

8.3. Circular Dichroism Spectral Studies

The CD spectrum[162] of the RNG-U_5·DNA-A_5 duplex exhibits B-form characteristics similar to those of the DNA-T_5·DNA-A_5 duplex. This result agrees with our molecular modeling studies that show that the overall structure of RNG is equilibrated in a B-DNA conformation.[114] However, the CD spectrum of RNG-U_5·RNA-A_5 differs from that of both RNA-U_5·RNA-A_5 (reference A-form; C′-3-endo) and DNA-T_5·DNA-A_5 (reference

dx.doi.org/10.1021/cr1004265 |*Chem. Rev.* 2012, 112, 1284–1309

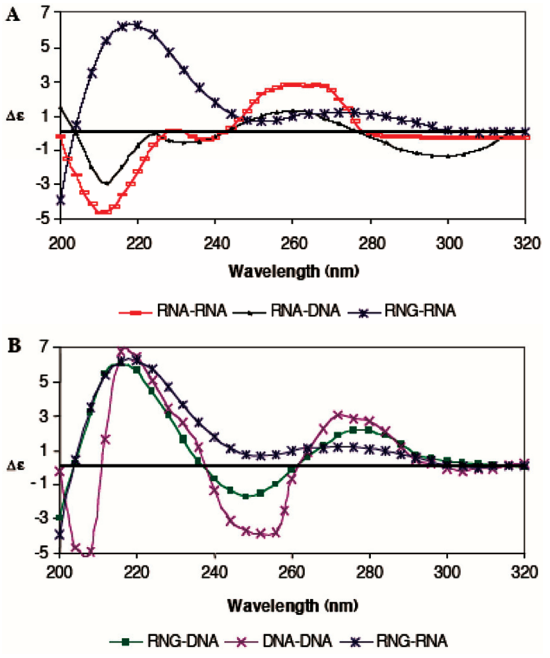

Figure 27. (A) The CD spectra of RNG-U_5·RNA-A_5 (blue), RNA-U_5·RNA-A_5 (red), and RNA-U_5·DNA-A_5 (black) (reference A-form). (B) The CD spectra of RNG-U_5·RNA-A_5 (blue), DNA-T_5·DNA-A_5 (magenta), and RNG-U_5·DNA-A_5 (green) (reference B-form). [oligomer] = 4 μM, pH 7.0, μ = 0.12 M). Reprinted with permission from ref 162. Copyright 2006 Elsevier.

B-form; C′-2-endo) (Figure 27). These changes may imply changes in the torsional angles of the guanidinium groups of the RNG-U_5 strand and the winding angle for RNA-A_5 duplexed with RNG-U_5. Although the structural changes cause RNG-U_5·RNA-A_5 to be less stable than RNA-U_5·RNA-A_5, it is more stable than the RNA-U_5·DNA-A_5, which has a standard A-form.

8.4. Molecular Dynamic Simulations

Molecular dynamic studies show that RNG-U_{12}·RNA-A_{12} has a conformation between that of the A- and B-forms.[163] The most important feature of the duplex is the very large propeller value (the dihedral angle between the base planes is $-45 \pm 9°$ compared to values of -14 to $-22°$ for native RNA, Figure 28).[162] The large propeller value can be explained from the tendency of the RNG backbone to adopt a more elongated structure rather than the compact A-form usually observed in RNA. The sp^3 phosphorus atoms of the phosphodiester groups in RNA cause the backbone to be very flexible, allowing for a more compact structure. In contrast, the sp^2 carbons of the guanidinium groups of RNG are rigid and locked in a planar conformation.

Simulation studies of RNA·RNA and RNG·RNA show that in RNA·RNA, the $P_n \cdots\cdots P_{n+1}$ distances are 5.9 ± 0.4 Å, which are normal for the A-form. In RNG·RNA, the $P_n \cdots\cdots P_{n+1}$ distances of the RNA strand are 6.0 ± 0.3 Å (again, typical of the A-form), but the $(C_n \cdots\cdots C_{n+1})$ distances between two RNG's units in the RNG strand are significantly longer (6.6 ± 0.2 Å), similar to a normal B-form. To compensate for this difference in strand length, RNG·RNA exhibits a large amount of propeller; it has been suggested that this reduces intrastrand clashes.[164]

Normally, two hydrogen bonds exist between U6 and A7 (at atoms N3····N1 and O4·····N6; Figure 29). The large amount of propeller causes the O4·····N6 hydrogen bond (shown in green) to break; O4 then forms a hydrogen bond with N6 of the

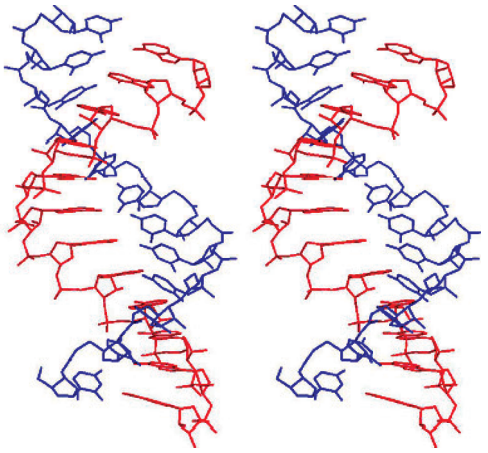

Figure 28. A stereoview of a MD simulated 1−5 ns averaged structure of the RNG-U_{12}·RNG-A_{12} duplex (the RNG strand is blue; RNA strand is red). The structure displays high levels of propeller, which are especially apparent in the center of this heavy-atom image. Reprinted with permission from ref 162. Copyright 2006 Elsevier.

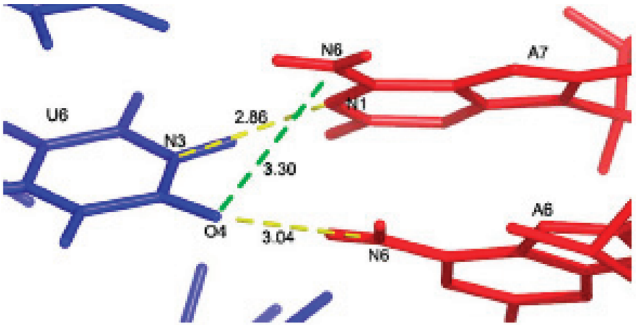

Figure 29. A close up view of the RNG-U_5·RNA-A_5 at 2−5 ns averaged structure with the RNG strand in blue and the RNA strand in red. Relevant residues, atoms, and potential heavy atom hydrogen-bonding distances, in Å, are labeled. Reprinted with permission from ref 162. Copyright 2006 Elsevier.

previous nucleotide, in this case A6. The modified hydrogen-bonding network increases the rigidity of the duplex, because each nucleotide is now bonded to two nucleotides. Although this hydrogen-bonding pattern partially compensates for loss of the natural hydrogen bond, it is not expected to be as stable as the natural Watson−Crick pattern. This explains the poor thermal stability of RNG-U_5·RNA-A_5 compared to that of RNA-U_5·RNA-A_5. The rigid B-form of RNG can bind tightly to B-DNA but not to A-RNA. Thus, RNG can differentiate between RNA and DNA.

The selective binding of RNG to DNA can be exploited for gene silencing by selective binding to DNA transcriptional sites, thereby inhibiting TF-protein·DNA complex formation without any unwanted binding to noncoding RNA.[165]

9. SUMMARY

Since the appearance of the first antisense drug, Formivirsen (Vitravene) in 1978, numerous compounds have been offered as therapeutic antisense/antigene agents directed toward viral infections and cancer. For effective inhibition of genetic expression at the level of transcription or translation, synthetic agents require cellular uptake, stability against nuclease degradation in vivo, lack of toxicity, and a strong binding affinity and high specificity toward the target DNA or RNA. We describe many

dx.doi.org/10.1021/cr1004265 |*Chem. Rev.* 2012, 112, 1284–1309

chemically modified oligonucleotides that have been studied. Central to our interest are those oligonucleotides in which the negatively charged phosphodiester linkages of DNA or RNA have been replaced by positively charged guanidinium and *S*-methylthiourea linkages, referred to as DNG and DNmt, respectively. The achiral nature of guanidinium and *S*-methylthiourea groups avoids stereoisomeric complexity.

Both DNG and DNmt have been shown to bind to DNA with Watson−Crick base-pair specificity. Because of the positive charges on DNG and the negative charges on DNA, the free energies of formation of duplex DNG·DNA and triplex DNG·DNA·DNG in aqueous solution are much greater than the free energies of formation of duplex DNA·DNA and triplex DNA·DNA·DNA under the same conditions. Of biological interest is the fact that DNG·DNA and DNG·DNA·DNG structures are most stable at physiological pH and ionic strength, whereas DNA·DNA and DNA·DNA·DNA are at minimum stability under these conditions (Figure 11). The synthesis of DNG, DNmt, and oligionuleotides with mixed backbones has been described.

Synthetic oligonucleotides that target either the 3′-end of the telomere or the RNA template of telomerase could potentially disrupt extension of the telomere that occurs during each cycle of cell divison. This technology is of interest in cancer research because lengthening of the telomere during cell division has been associated with the immortality of cancerous cells. Complementary DNGs have been found to bind tightly to telomeric sequences. DNG binds to both DNA and RNA, but exhibits a marked preference for RNA. Complementary DNGs have also been found to bind to the ATATAT sequence that is common in *Plasmodium falciparum*, the protozoan responsible for malaria.

The introduction of cationic linkages in the oligonucleotide backbone could potentially overcome the need to use cationic vectors to facilitate cellular uptake. Results from DNG and DNmt, as well as from DNG/DNA and RNG/DNA chimeras, show that they are stable toward nucleases. Thus, both DNG and DNmt oligonucleotides offer a new dimension to the existing antisense/antigene approach.

AUTHOR INFORMATION

Corresponding Author

*E-mail: tcbruice@chem.ucsb.edu.

BIOGRAPHIES

Moti L. Jain received his Ph.D. in organic chemistry in 1991 with Jagdish P. Saxena at the University of Jodhpur in Rajasthan, India. After working with Jih Ru-Hwu at Academia Sinica, Taipei, Taiwan, he worked with Ken Turnbull and David Vicic at the University of Arkansas as postdoctoral fellow (2001−2003) before joining Thomas C. Bruice's group in 2003. From 2007−2009, he worked as a Senior Scientist at Osmetech Molecular Diagnostics and Life Technologies. He is currently working as a Senior Manager of Chemistry at Centrillion Biosciences in Mountain View, California.

Paula Yurkanis Bruice received an A.B. from Mount Holyoke College and a Ph.D. in organic chemistry from the University of Virginia. She received an NIH postdoctoral fellowship for study in the Department of Biochemistry at the University of Virginia Medical School and held a postdoctoral appointment in the Department of Pharmacology at Yale Medical School. She has been a member of the faculty at the University of California, Santa Barbara since 1972. She is the author of *Organic Chemistry* and *Essentials of Organic Chemistry*.

István E. Szabó was born in Los Angeles, California. He joined Thomas C. Bruice's research group as an undergraduate and earned a B.S. in Biochemistry from the University of California, Santa Barbara where he is currently a graduate student in the Department of Chemistry and Biochemistry.

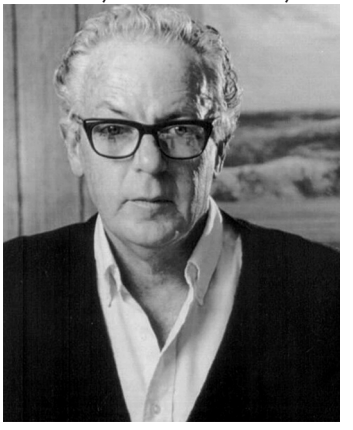

Thomas C. Bruice received a B.S. and Ph.D. degrees from the University Southern California and served as a National Research Council postdoctoral fellow in chemistry at UCLA. He has served on the faculties of Yale School of Medicine, Johns Hopkins School of Medicine, and Cornell University. He is currently a Research Professor at the University of California, Santa Barbara. He is a member of the National Academy of Science (USA), the American Academy of Arts and Science, and a Fellow of the Royal Society of Chemistry. His major Awards include the Chemistry Medal of the National Academy of Science and the Linus Pauling Medal. American Chemical Society awards include the Bader Award in bioorganic chemistry, the James Flack Norris Award in physical organic chemistry, and the Repligen Award in biochemistry.

ACKNOWLEDGMENT

Work from our laboratory, cited in this review, has been partially supported by the National Institutes of Health. We are grateful to the many co-workers and collaborators who have contributed to this research. We also thank Dr. Myunji Park for her help in preparing the manuscript.

REFERENCES

(1) Zamecnik, P. C.; Stephenson, M. L. *Proc. Natl. Acad. Sci. U. S. A.* **1978**, *75*, 280.
(2) Kurreck, J. *Eur. J. Biochem.* **2003**, *270*, 1628.
(3) Chan, J. H.; Lim, S.; Wong, W. F. *Clin. Exp. Pharmacol. Physiol.* **2006**, *33*, 533.
(4) Dean, N. M.; Bennett, C. F. *Oncogene* **2003**, *22*, 9087.
(5) Fichou, Y.; Férec, C. *Trends Biotechnol.* **2006**, *24*, 563.
(6) Gleave, M. E.; Monia, B. P. *Nat. Rev. Cancer* **2005**, *5*, 468.
(7) Rayburn, E. R.; Zhang, R. *Drug Discovery Today* **2008**, *13*, 513.
(8) Van Aerschot, A. *Antiviral Res.* **2006**, *71*, 307.
(9) Vidal, L.; Blagden, S.; Attard, G.; de Bono, J. *Eur. J. Cancer* **2005**, *41*, 2812.
(10) Zhang, Y. C.; Taylor, M. M.; Samson, W. K.; Phillips, M. I. In *Antisense Therapeutics*; Humana Press: Totowa, 2005; p 11.
(11) Armitage, B. A. *Nat. Chem. Biol.* **2005**, *1*, 185.
(12) Elbashir, S. M.; Harborth, J.; Lendeckel, W.; Yalcin, A.; Weber, K.; Tuschl, T. *Nature* **2001**, *411*, 494.
(13) Fire, A.; Xu, S.; Montgomery, M. K.; Kostas, S. A.; Driver, S. E.; Mello, C. C. *Nature* **1998**, *391*, 806.
(14) Bumcrot, D.; Manoharan, M.; Koteliansky, V.; Sah, D. W. Y. *Nat Chem Biol* **2006**, *2*, 711.
(15) Gaither, A.; Iourgenko, V. *Curr. Opin. Oncol.* **2007**, *19*, 50.
(16) Jain, K. K. *Mol. BioSystems* **2006**, *2*, 523.
(17) Takeshita, F.; Ochiya, T. *Cancer Sci.* **2006**, *97*, 689.
(18) Kurreck, J.; Wyszko, E.; Gillen, C.; Erdmann, V. A. *Nucleic Acids Res.* **2002**, *30*, 1911.
(19) Juliano, R.; Bauman, J.; Kang, H.; Ming, X. *Mol. Pharmaceutics* **2009**, *6*, 686.
(20) Mansoor, M.; Melendez, A. J. *Gene Regul. Syst. Biol.* **2008**, *2*, 275.
(21) Crooke, S. T. *Methods Enzymol.* **2000**, *313*, 3.
(22) Levin, A. A. *Biochim. Biophys. Acta* **1999**, *1489*, 69.
(23) Cook, P. D. *Annu. Rep. Med. Chem.* **1998**, *33*, 313.
(24) Agrawal, S.; Zhao, Q. *Antisense Nucleic Acid Drug Dev.* **1998**, *8*, 135.
(25) Goel, S.; Desai, K.; Bulgaru, A.; Fields, A.; Goldberg, G.; Agrawal, S.; Martin, R.; Grindel, M.; Mani, S. *Clin. Cancer. Res.* **2003**, *9*, 4069.
(26) Shen, L. X.; Kandimalla, E. R.; Agrawal, S. *Bioorg. Med. Chem.* **1998**, *6*, 1695.
(27) Elayadi, A.; Corey, D. *Curr. Opin. Investigational Drugs* **2001**, *2*, 558.
(28) Nielsen, P. *Mol. Biotechnol.* **2004**, *26*, 233.
(29) Nielsen, P. E.; Egholm, M. *Curr. Issues Mol. Biol.* **1999**, *1*, 89.
(30) Heasman, J. *Dev. Biol.* **2002**, *243*, 209.
(31) Summerton, J. *Biochim. Biophys. Acta, Gene Struct. Expression* **1999**, *1489*, 141.
(32) Braasch, D. A.; Corey, D. R. *Chem. Biol.* **2001**, *8*, 1.
(33) Crinelli, R.; Bianchi, M.; Gentilini, L.; Palma, L.; Magnani, M. *Curr. Drug Targets* **2004**, *5*, 745.
(34) K. Singh, S.; A. Koshkin, A.; Wengel, J.; Nielsen, P. *Chem. Commun.* **1998**, 455.
(35) Obika, S.; Nanbu, D.; Hari, Y.; Andoh, J.-i.; Morio, K.-i.; Doi, T.; Imanishi, T. *Tetrahedron Lett.* **1998**, *39*, 5401.
(36) Obika, S.; Nanbu, D.; Hari, Y.; Morio, K.-i.; In, Y.; Ishida, T.; Imanishi, T. *Tetrahedron Lett.* **1997**, *38*, 8735.
(37) Bondensgaard, K.; Petersen, M.; Singh, S. K.; Rajwanshi, V. K.; Kumar, R.; Wengel, J.; Jacobsen, J. P. *Chem.—Eur. J.* **2000**, *6*, 2687.
(38) Faria, M.; Spiller, D. G.; Dubertret, C.; Nelson, J. S.; White, M. R. H.; Scherman, D.; Helene, C.; Giovannangeli, C. *Nat. Biotechnol.* **2001**, *19*, 40.
(39) Gryaznov, S.; Chen, J.-K. *J. Am. Chem. Soc.* **1994**, *116*, 3143.
(40) Leumann, C. J. *CHIMIA Int. J. Chem.* **2001**, *55*, 1041.
(41) Renneberg, D.; Bouliong, E.; Reber, U.; Schumperli, D.; Leumann, C. J. *Nucleic Acids Res.* **2002**, *30*, 2751.
(42) Gu, P.; Schepers, G.; Rozenski, J.; Van Aerschot, A.; Herdewijn, P. *Oligonucleotides* **2003**, *13*, 479.
(43) Wang, J.; Verbeure, B.; Luyten, I.; Froeyen, M.; Hendrix, C.; Rosemeyer, H.; Seela, F.; Van Aerschot, A.; Herdewijn, P. *Nucleosides, Nucleotides, Nucleic Acids* **2001**, *20*, 785.
(44) Hughes, J.; Astriab, A.; Yoo, H.; Alahari, S.; Liang, E.; Sergueev, D.; Shaw, B. R.; Juliano, R. L. *Methods Enzymol.* **2000**, *313*, 342.
(45) Tari, A. M. *Methods Enzymol.* **2000**, *313*, 372.
(46) Delong, R.; Stephenson, K.; Loftus, T.; Fisher, M.; Alahari, S.; Nolting, A.; Juliano, R. L. *J. Pharm. Sci.* **1997**, *86*, 762.
(47) Patil, S.; Rhodes, D.; Burgess, D. *AAPS J.* **2005**, *7*, E61.
(48) Barawkar, D.; Rajeev, K.; Kumar, V.; Ganesh, K. *Nucleic Acids Res.* **1996**, *24*, 1229.
(49) Bijapur, J.; Keppler, M.; Bergqvist, S.; Brown, T.; Fox, K. *Nucleic Acids Res.* **1999**, *27*, 1802.
(50) Robles, J.; Grandas, A.; Pedroso, E. *Tetrahedron* **2001**, *57*, 179.
(51) Roig, V.; Asseline, U. *J. Am. Chem. Soc.* **2003**, *125*, 4416.
(52) Ueno, Y.; Mikawa, M.; Matsuda, A. *Bioconj. Chem.* **1998**, *9*, 33.
(53) Cuenoud, B.; Casset, F.; Hüsken, D.; Natt, F.; Wolf, R. M.; Altmann, K.-H.; Martin, P.; Moser, H. E. *Angew. Chem., Int. Ed.* **1998**, *37*, 1288.
(54) Kanazaki, M.; Ueno, Y.; Shuto, S.; Matsuda, A. *J. Am. Chem. Soc.* **2000**, *122*, 2422.
(55) Prakash, T. P.; Manoharan, M.; Fraser, A. S.; Kawasaki, A. M.; Lesnik, E. A.; Owens, S. R. *Tetrahedron Lett.* **2000**, *41*, 4855.
(56) Puri, N.; Majumdar, A.; Cuenoud, B.; Natt, F.; Martin, P.; Boyd, A.; Miller, P. S.; Seidman, M. M. *Biochemistry (Moscow)* **2002**, *41*, 7716.
(57) Bailey, C.; Dagle, J.; Weeks, D. *Nucleic Acids Res.* **1998**, *26*, 4860.
(58) Chaturvedi, S.; Horn, T.; Letsinger, R. *Nucleic Acids Res.* **1996**, *24*, 2318.
(59) Dagle, J. M.; Littig, J. L.; Sutherland, L. B.; Weeks, D. L. *Nucleic Acids Res.* **2000**, *28*, 2153.
(60) Kore, A.; Salunkhe, M. *Ind. J. Chem. Sect. B* **1998**, *37*, 536.
(61) Letsinger, R. L.; Singman, C. N.; Histand, G.; Salunkhe, M. *J. Am. Chem. Soc.* **1988**, *110*, 4470.
(62) Michel, T.; Debart, F.; Vasseur, J.-J. *Tetrahedron Lett.* **2003**, *44*, 6579.
(63) Robles, J.; Ibáñez, V.; Grandas, A.; Pedroso, E. *Tetrahedron Lett.* **1999**, *40*, 7131.
(64) Vasquez, K. M.; Dagle, J. M.; Weeks, D. L.; Glazer, P. M. *J. Biol. Chem.* **2001**, *276*, 38536.
(65) Fox, K. R. *Curr. Med. Chem.* **2000**, *7*, 17.

(66) Lebedev, A.; Wickstrom, E. *Perspect. Drug Discovery Des.* **1996**, *4*, 17.
(67) Zhou, P.; Wang, M.; Du, L.; Fisher, G. W.; Waggoner, A.; Ly, D. H. *J. Am. Chem. Soc.* **2003**, *125*, 6878.
(68) Moulton, J.; Jiang, S. *Molecules* **2009**, *14*, 1304.
(69) Perreault, D. M.; Cabell, L. A.; Anslyn, E. V. *Bioorg. Med. Chem.* **1997**, *5*, 1209.
(70) Wilds, C. J.; Maier, M. A.; Tereshko, V.; Manoharan, M.; Egli, M. *Angew. Chem., Int. Ed. Engl.* **2002**, *41*, 115.
(71) Prakash, T. P.; Püschl, A.; Lesnik, E.; Mohan, V.; Tereshko, V.; Egli, M.; Manoharan, M. *Org. Lett.* **2004**, *6*, 1971.
(72) Deglane, G.; Abes, S.; Michel, T.; Prévot, P.; Vives, E.; Debart, F.; Barvik, I.; Lebleu, B.; Vasseur, J.-J. *Chem. Biochem.* **2006**, *7*, 684.
(73) Barawkar, D. A.; Linkletter, B.; Bruice, T. C. *Bioorg. Med. Chem. Lett.* **1998**, *8*, 1517.
(74) Blasko, A.; Dempcy, R. O.; Minyat, E. E.; Bruice, T. C. *J. Am. Chem. Soc.* **1996**, *118*, 7892.
(75) Blasko, A.; Minyat, E. E.; Dempcy, R. O.; Bruice, T. C. *Biochemistry (Moscow)* **1997**, *36*, 7821.
(76) Browne, K. A.; Dempcy, R. O.; Bruice, T. C. *Proc. Natl. Acad. Sci. U. S. A.* **1995**, *92*, 7051.
(77) Challa, H.; Bruice, T. C. *Bioorg. Med. Chem.* **2004**, *12*, 1475.
(78) Dempcy, R. O.; Almarsson, O.; Bruice, T. C. *Proc. Natl. Acad. Sci. U. S. A.* **1994**, *91*, 7864.
(79) Dempcy, R. O.; Browne, K. A.; Bruice, T. C. *Proc. Natl. Acad. Sci. U. S. A.* **1995**, *92*, 6097.
(80) Dempcy, R. O.; Browne, K. A.; Bruice, T. C. *J. Am. Chem. Soc.* **1995**, *117*, 6140.
(81) Linkletter, B. A.; Szabo, I. E.; Bruice, T. C. *J. Am. Chem. Soc.* **1999**, *121*, 3888.
(82) Reddy, P. M.; Bruice, T. C. *Bioorg. Med. Chem. Lett.* **2003**, *13*, 1281.
(83) Linkletter, B. A.; Bruice, T. C. *Bioorg. Med. Chem. Lett.* **1998**, *8*, 1285.
(84) Kim, S. K.; Nielsen, P. E.; Egholm, M.; Buchardt, O.; Berg, R. H.; Norden, B. *J. Am. Chem. Soc.* **1993**, *115*, 6477.
(85) Robinson, S.; Roskamp, E. J. *Tetrahedron* **1997**, *53*, 6697.
(86) Linkletter, B. A.; Szabo, I. E.; Bruice, T. C. *Nucleic Acids Res.* **2001**, *29*, 2370.
(87) Czernecki, S.; Valery, J.-M. *J. Chem. Soc., Chem. Commun.* **1990**, *11*, 801.
(88) Hansske, F.; Robins, M. J. *J. Am. Chem. Soc.* **1983**, *105*, 6736.
(89) Wagner, D.; Verheyden, J. P. H.; Moffatt, J. G. *J. Org. Chem.* **1974**, *39*, 24.
(90) Jain, M. L.; Bruice, T. C. *Bioorg. Med. Chem.* **2006**, *14*, 7333.
(91) Kearney, P. C.; Fernandez, M.; Flygare, J. A. *J. Org. Chem.* **1998**, *63*, 196.
(92) Szabo, I. E.; Bruice, T. C. *Bioorg. Med. Chem.* **2004**, *12*, 4233.
(93) Uzagare, M. C.; Sanghvi, Y. S.; Salunkhe, M. M. *Synth. Commun.* **2004**, *34*, 1071.
(94) Jones, G.; Manczak, M.; Schelling, D.; Turner, H.; Jones, D. *Biochem. J.* **1998**, *335*, 79.
(95) Park, M.; Bruice, T. C. *Bioorg. Med. Chem. Lett.* **2008**, *18*, 3488.
(96) Olaussen, K. A.; Dubrana, K.; Domont, J.; Spano, J.-P.; Sabatier, L.; Soria, J.-C. *Crit. Rev. Oncol./Hematol.* **2006**, *57*, 191.
(97) Matthes, E.; Lehmann, C. *Nucleic Acids Res.* **1999**, *27*, 1152.
(98) Norton, J. C.; Piatyszek, M. A.; Wright, W. E.; Shay, J. W.; Corey, D. R. *Nat. Biotechnol.* **1996**, *14*, 615.
(99) Gryaznov, S.; Pongracz, K.; Matray, T.; Schultz, R.; Pruzan, R.; Aimi, J.; Chin, A.; Harley, C.; Shea-Herbert, B.; Shay, J.; Oshima, Y.; Asai, A.; Yamashita, Y. *Nucleosides, Nucleotides Nucleic Acids* **2001**, *20*, 401.
(100) Pitts, A. E.; Corey, D. R. *Proc. Natl. Acad. Sci. U. S. A.* **1998**, *95*, 11549.
(101) Neidle, S.; Parkinson, G. *Nat. Rev. Drug Discovery* **2002**, *1*, 383.
(102) Hochreiter, A. E.; Xiao, H.; Goldblatt, E. M.; Gryaznov, S. M.; Miller, K. D.; Badve, S.; Sledge, G. W.; Herbert, B.-S. *Clin. Cancer. Res.* **2006**, *12*, 3184.
(103) Makarov, V. L.; Hirose, Y.; Langmore, J. P. *Cell* 1997, *88*, 657.
(104) Zhang, X.; Bruice, T. C. *Bioorg. Med. Chem. Lett.* **2008**, *18*, 665.
(105) Lee, M. S.; Feig, M.; F. R., S., Jr.; C. L., B., III *J. Comput. Chem.* **2003**, *24*, 1348.
(106) Lee, M. S.; Salsbury, F. R., Jr.; Brooks, C. L., III *J. Chem. Phys.* **2002**, *116*, 10606.
(107) Lei, M.; Zaug, A. J.; Podell, E. R.; Cech, T. R. *J. Biol. Chem.* **2005**, *280*, 20449.
(108) Park, M.; Bruice, T. C. *Bioorg. Med. Chem. Lett.* **2010**, *20*, 3982.
(109) Arya, D. P.; Bruice, T. C. *J. Am. Chem. Soc.* **1998**, *120*, 6619.
(110) Arya, D. P.; Bruice, T. C. *J. Am. Chem. Soc.* **1998**, *120*, 12419.
(111) Arya, D. P.; Bruice, T. C. *Proc. Natl. Acad. Sci. U. S. A.* **1999**, *96*, 4384.
(112) Arya, D. P.; Bruice, T. C. *J. Am. Chem. Soc.* **1999**, *121*, 10680.
(113) Arya, D. P.; Bruice, T. C. *Bioorg. Med. Chem. Lett.* **2000**, *10*, 691.
(114) Luo, J.; Bruice, T. C. *J. Am. Chem. Soc.* **1998**, *120*, 1115.
(115) Luo, J.; Bruice, T. C. *J. Biomol. Struct. Dyn.* **2000**, *17*, 629.
(116) Kim, J.; Klooster, S.; Shapiro, D. J. *J. Biol. Chem.* **1995**, *270*, 1282.
(117) Perez-Martin, J.; Rojo, F.; de Lorenzo, V. *Microbiol. Mol. Biol. Rev.* **1994**, *58*, 268.
(118) Raghunathan, G.; Miles, H. T.; Sasisekharan, V. *Biochemistry (Moscow)* **1993**, *32*, 455.
(119) UCSF Computer Graphics Laboratory, 1997.
(120) Lennox, K. A.; Sabel, J. L.; Johnson, M. J.; Moreira, B. G.; Fletcher, C. A.; Rose, S. D.; Behlke, M. A.; Laikhter, A. L.; Walder, J. A.; Dagle, J. M. *Oligonucleotides* **2006**, *16*, 26.
(121) Pirollo, K. F.; Rait, A.; Sleer, L. S.; Chang, E. H. *Pharmacol. Ther.* **2003**, *99*, 55.
(122) Chen, H. X.; Marshall, J. L.; Ness, E.; Martin, R. R.; Dvorchik, B.; Rizvi, N.; Marquis, J.; McKinlay, M.; Dahut, W.; Hawkins, M. J. *Clin. Cancer. Res.* **2000**, *6*, 1259.
(123) Geary, R. S.; Yu, R. Z.; Watanabe, T.; Henry, S. P.; Hardee, G. E.; Chappell, A.; Matson, J.; Sasmor, H.; Cummins, L.; Levin, A. A. *Drug Metab. Dispos.* **2003**, *31*, 1419.
(124) Sewell, K. L.; Geary, R. S.; Baker, B. F.; Glover, J. M.; Mant, T. G. K.; Yu, R. Z.; Tami, J. A.; Dorr, F. A. *J. Pharmacol. Exp. Ther.* **2002**, *303*, 1334.
(125) Wang, H.; Cai, Q.; Zeng, X.; Yu, D.; Agrawal, S.; Zhang, R. *Proc. Natl. Acad. Sci. U. S. A.* **1999**, *96*, 13989.
(126) Barawkar, D. A.; Bruice, T. C. *Proc. Natl. Acad. Sci. U. S. A.* **1998**, *95*, 11047.
(127) Challa, H.; Bruice, T. C. *Bioorg. Med. Chem. Lett.* **2001**, *11*, 2423.
(128) Job, P. *Ann. Chim.* **1928**, *10*, 113.
(129) Barawkar, D. A.; Bruice, T. C. *J. Am. Chem. Soc.* **1999**, *121*, 10418.
(130) Barawkar, D. A.; Kwok, Y.; Bruice, T. W.; Bruice, T. C. *J. Am. Chem. Soc.* **2000**, *122*, 5244.
(131) Hyrup, B.; Nielsen, P. E. *Bioorg. Med. Chem.* **1996**, *4*, 5.
(132) Buchardt, O.; Egholm, M.; Berg, R. H.; Nielsen, P. E. *Trends Biotechnol.* **1993**, *11*, 384.
(133) Wittung, P.; Kajanus, J.; Edwards, K.; Nielsen, P.; Nordén, B.; Malmström, B. G. *FEBS Lett.* **1995**, *365*, 27.
(134) Ray, A.; Norden, B. *FASEB J.* **2000**, *14*, 1041.
(135) Hanvey, J.; Peffer, N.; Bisi, J.; Thomson, S.; Cadilla, R.; Josey, J.; Ricca, D.; Hassman, C.; Bonham, M.; Au, K.; Carter, S. G.; Bruckenstein, D. A.; Boyd, A. L.; Noble, S. A.; Babiss, L. E. *Science* **1992**, *258*, 1481.
(136) Cutrona, G.; Carpaneto, E. M.; Ulivi, M.; Roncella, S.; Landt, O.; Ferrarini, M.; Boffa, L. C. *Nat. Biotechnol.* **2000**, *18*, 300.
(137) Finn, P.; Gibson, N.; Fallon, R.; Hamilton, A.; Brown, T. *Nucleic Acids Res.* **1996**, *24*, 3357.
(138) Reddy, P. M.; Bruice, T. C. *J. Am. Chem. Soc.* **2004**, *126*, 3736.
(139) Thuong, N. T.; Asseline, U.; Montenay-Garestier, T. In *Oligonucleotides as Inhibitors of Gene Expression in Topics (In Molecular and Structural Biology)*; Cohen, J. S., Ed.; MacMillan Press: Boca Raton, 1989; p 12.

(140) Lemaitre, M.; Bayard, B.; Lebleu, B. *Proc. Natl. Acad. Sci. U. S. A.* **1987**, *84*, 648.
(141) Rajur, S. B.; Robles, J.; Wiederholt, K.; Kuimelis, R. G.; McLaughlin, L. W. *J. Org. Chem.* **1997**, *62*, 523.
(142) Robles, J.; McLaughlin, L. W. *J. Am. Chem. Soc.* **1997**, *119*, 6014.
(143) Wiederholt, K.; Rajur, S. B.; Giuliano, J.; O'Donnel, M. J.; McLaughlin, L. W. *J. Am. Chem. Soc.* **1996**, *118*, 7055.
(144) Escudé, C.; Nguyen, C. H.; Kukreti, S.; Janin, Y.; Sun, J.-S.; Bisagni, E.; Garestier, T.; Hélène, C. *Proc. Natl. Acad. Sci. U. S. A.* **1998**, *95*, 3591.
(145) Fox, K. R.; Polucci, P.; Jenkins, T. C.; Neidle, S. *Proc. Natl. Acad. Sci. U. S. A.* **1995**, *92*, 7887.
(146) Lee, J. S.; Latimer, L. J. P.; Hampel, K. J. *Biochemistry (Moscow)* **1993**, *32*, 5591.
(147) Mergny, J. L.; Duval-Valentin, G.; Nguyen, C. H.; Perrouault, L.; Faucon, B.; Rougee, M.; Montenay-Garestier, T.; Bisagni, E.; Helene, C. *Science* **1992**, *256*, 1681.
(148) Wilson, W. D.; Tanious, F. A.; Mizan, S.; Yao, S.; Kiselyov, A. S.; Zon, G.; Strekowski, L. *Biochemistry (Moscow)* **1993**, *32*, 10614.
(149) Araki, T.; Yamamoto, A.; Yamada, M. *Histochem. Cell Biol.* **1987**, *87*, 331.
(150) Comings, D. E. *Chromosoma* **1975**, *52*, 229.
(151) Karawajew, L.; Rudchenko, S.; Wlasik, T.; Trakht, I.; Rakitskaya, V. *J. Immunol. Methods* **1990**, *129*, 277.
(152) Sterzel, W.; Bedford, P.; Eisenbrand, G. *Anal. Biochem.* **1985**, *147*, 462.
(153) Weisblum, B.; Haenssler, E. *Chromosoma* **1974**, *46*, 255.
(154) Arndt-Jovin, D. J.; Jovin, T. M. *Cytometry* **1990**, *11*, 80.
(155) Frau, S.; Bernadou, J.; Meunier, B. *Bull. Soc. Chim. Fr.* **1996**, *133*, 1053.
(156) Holmquist, G. *Chromosoma* **1975**, *49*, 333.
(157) Argentini, M.; Dos Santos, D. F.; Weinreich, R.; Hansen, H.-J. *Inorg. Chem.* **1998**, *37*, 6018.
(158) Dempcy, R. O.; Luo, J.; Bruice, T. C. *Proc. Natl. Acad. Sci. U. S. A.* **1996**, *93*, 4326.
(159) Kojima, N.; Bruice, T. C. *Org. Lett.* **2000**, *2*, 81.
(160) Kojima, N.; Szabo, I. E.; Bruice, T. C. *Tetrahedron* **2002**, *58*, 867.
(161) Park, M.; Bruice, T. C. *Bioorg. Med. Chem. Lett.* **2005**, *15*, 3247.
(162) Park, M.; Toporowski, J. W.; Bruice, T. C. *Bioorg. Med. Chem.* **2006**, *14*, 1743.
(163) Conte, M.; Conn, G.; Brown, T.; Lane, A. *Nucleic Acids Res.* **1997**, *25*, 2627.
(164) Calladine, C. R. *J. Mol. Biol.* **1982**, *161*, 343.
(165) Willingham, A. T.; Orth, A. P.; Batalov, S.; Peters, E. C.; Wen, B. G.; Aza-Blanc, P.; Hogenesch, J. B.; Schultz, P. G. *Science* **2005**, *309*, 1570.